The method of projected characteristics for the evolution of magnetic arches

Article *in* Astronomy and Astrophysics · July 1987

Source: NTRS

S. T. Wu
University of Alabama in Huntsville

Astron. Astrophys. 179, 354–370 (1987)

ASTRONOMY AND ASTROPHYSICS

The method of projected characteristics for the evolution of magnetic arches

Y. Nakagawa[1]★, Y.Q. Hu[2]★★, and S.T. Wu[2]

[1] Chiba Institute of Technology, Narashino 274, Japan
[2] The University of Alabama in Huntsville, Huntsville, AL 35899, USA

Received May 29, 1985; accepted November 26, 1986

Summary. A numerical method of solving fully nonlinear MHD equation is described. In particular, the formulation based on the newly developed method of projected characteristics (Nakagawa, 1981a,b) suitable to study the evolution of magnetic arches due to motions of their foot-points is presented. The final formulation is given in the form of difference equations, therefore, the analysis of numerical stability is also presented. Further, the most important derivation of physically self-consistent, time-dependent boundary conditions (i.e., the evolving boundary equations) is given in detail, and some results obtained with such boundary equations are reported.

Key words: hydromagnetics – Sun – magnetic field evolution

1. Introduction

A large class of astrophysical phenomena, such as flares on the Sun and X-ray bursts on some stars, are considered as consequences of evolving atmospheric magnetic fields. In a previous series of papers (Nakagawa, 1980, 1981a,b), it has been shown that these problems can be treated by the method of projected characteristics. However, the details of the method have never been presented, therefore, in this paper, the basic idea is described together with the formulations suitable to study the evolution of magnetic arches due to motions of their foot-points.

The basic equations of magnetohydrodynamics (MHD) are the laws of conservation of mass, momentum and energy, supplemented by the induction equation of magnetic field. This system of equations is hyperbolic; therefore, it is possible to obtain solutions by the method of characteristics. Nevertheless, direct application of the method of characteristics to a problem more than one-spatial dimension becomes an exceedingly complicated numerical procedure due to the non-isotropic nature of magnetohydrodynamic waves as shown by Sauerwein (1966). Accordingly, the method of projected characteristics was developed by Nakagawa (1981a,b) to circumvent this complexity, while retaining physical insights into consequences of non-linear interactions. The basic idea of the approach is described in Sect. 2 and the summary of general formulation is presented in Sect. 3. The formulations are given in forms of difference equations for numerical study, thus the analysis of numerical stability is given in Sect. 4. In Sect. V the derivation of proper time-dependent boundary conditions (called the boundary equations) is described for a practical example of two-(spatial) dimensional problem. Some numerical results obtained by the use of only normal projected characteristics together with additional non-reflecting boundary conditions as suggested by FICE numerical scheme (Hu and Wu, 1984) for the induced wave and mass motion (Wu et al., 1983; 1986) and for flare energy build up (Wu et al. 1984) are illustrated in Sect. 6 and in the final Sect. 7 physical significance of the present formulation is discussed.

Send offprint requests to: S.T. Wu

★ Adjunct Professor, University of Alabama in Huntsville

★★ Visiting Scholar from China University of Science and Technology, Hefei, Anhui, People's Republic of China

2. Basic idea of the method of characteristics

2.1. Fundamental approach

A partial differential equation of a function $f(x,t)$ of two independent variables x and t

$$\frac{\partial f}{\partial t} + u\frac{\partial f}{\partial x} = g, \tag{1}$$

can be written as a total differential equation of the form

$$\frac{df}{ds} = g. \tag{2}$$

This transformation is possible as the definition of the directional derivative in the (x,t) plane along a curve $s(x,t)$ is

$$\frac{df}{ds} = \frac{\partial f}{\partial t}\frac{\partial t}{\partial s} + \frac{\partial f}{\partial x}\frac{\partial x}{\partial s}, \tag{3}$$

where the direction of the curve $s(x,t)$ is

$$\frac{dx}{dt} = -\frac{\partial s/\partial t}{\partial s/\partial x} = u \tag{4}$$

Thus, the solution of Eq. (1) can be obtained by integrating Eq. (2) along the curve $s(x,t)$ even for the nonlinear case of u and g being general functions of x and t in the form

$$f(s) = f(0) + \int_0^s g\,ds, \tag{5}$$

where $f(0)$ denotes the values of $f(x,t)$ at $s=0$.

This is the basic idea of the method of characteristics to obtain the solutions of nonlinear hyperbolic partial differential equations. The curves along which total differential equations can be derived are called the characteristics, while the resultant equations are called the compatibility equations. In practical MHD problems, various physical variables correspond to the function $f(x, t)$ and the compatibility equations can be obtained for combinations of physical variables along a number of characteristics even in the one (spatial) dimensional problem (see, for example, Akihiezer, et al., 1975). For a more general two or three dimensional problem, the characteristic curves are characteristic surfaces and the compatibility equations are complex differential equations as shown by Sauerwein (1966).

It should be noted that the existence of the integral of the type of Eq. (5) implies that physical variables at different times and positions are related by such an integral and the physical causality relation can be traced along the characteristic. Accordingly at the boundary, the time variation of the boundary condition must be treated properly in consideration of such a relationship: this relationship given in terms of specific compatibility equation is hereafter called the boundary equation.

2.2. *Characteristic surfaces for the general MHD problem*

In a system of cartesian coordinates (x, y, z) with the x and y axes in the horizontal plane and z axis along the vertical, the basic set of MHD equations for a perfectly conducting fluid can be written in the form

$$\frac{D\rho}{Dt} + \rho\frac{\partial u}{\partial x} + \rho\frac{\partial v}{\partial y} + \rho\frac{\partial w}{\partial z} = 0\,, \tag{6}$$

$$\frac{Du}{Dt} + \frac{1}{\rho}\frac{\partial p}{\partial x} + \frac{B_y}{\rho}\frac{\partial B_y}{\partial x} + \frac{B_z}{\rho}\frac{\partial B_z}{\partial x} - \frac{B_y}{\rho}\frac{\partial B_x}{\partial y} - \frac{B_z}{\rho}\frac{\partial B_x}{\partial z} = 0\,, \tag{7}$$

$$\frac{Dv}{Dt} + \frac{1}{\rho}\frac{\partial p}{\partial y} - \frac{B_x}{\rho}\frac{\partial B_y}{\partial x} + \frac{B_x}{\rho}\frac{\partial B_x}{\partial y} + \frac{B_z}{\rho}\frac{\partial B_z}{\partial y} - \frac{B_z}{\rho}\frac{\partial B_y}{\partial z} = 0\,, \tag{8}$$

$$\frac{Dw}{Dt} + \frac{1}{\rho}\frac{\partial p}{\partial z} - \frac{B_x}{\rho}\frac{\partial B_z}{\partial x} - \frac{B_y}{\rho}\frac{\partial B_z}{\partial y} + \frac{B_x}{\rho}\frac{\partial B_x}{\partial z} + \frac{B_y}{\rho}\frac{\partial B_y}{\partial z} = -g\,, \tag{9}$$

$$\frac{Dp}{Dt} + a^2\rho\left(\frac{\partial u}{\partial x} + \frac{\partial v}{\partial y} + \frac{\partial w}{\partial z}\right) = (\gamma - 1)\Delta Q\,, \tag{10}$$

$$\frac{DB_x}{Dt} - B_y\frac{\partial u}{\partial y} + B_x\frac{\partial v}{\partial y} - B_z\frac{\partial u}{\partial z} + B_x\frac{\partial w}{\partial z} = 0\,, \tag{11}$$

$$\frac{DB_y}{Dt} + B_y\frac{\partial u}{\partial x} - B_x\frac{\partial v}{\partial x} - B_z\frac{\partial v}{\partial z} + B_y\frac{\partial w}{\partial z} = 0\,, \tag{12}$$

$$\frac{DB_z}{Dt} + B_z\frac{\partial u}{\partial x} - B_x\frac{\partial w}{\partial x} + B_z\frac{\partial v}{\partial y} - B_y\frac{\partial w}{\partial y} = 0\,, \tag{13}$$

where

$$\frac{D}{Dt} = \frac{\partial}{\partial t} + u\frac{\partial}{\partial x} + v\frac{\partial}{\partial y} + w\frac{\partial}{\partial z}$$

In Eqs. (6)–(13), the variables are ρ the density, $\mathbf{v} = (u, v, w)$ the velocity, p the pressure, B_x, B_y and B_z the components of magnetic field induction in the unit of $\sqrt{\mu_0}$, with μ_0 being the magnetic permeability, g the gravitational acceleration, a the adiabatic speed of sound, γ the ratio of specific heats, and the term $(\gamma - 1)\Delta Q$ the net rate of irreversible energy (heat) gain or loss per unit volume. The three thermodynamic variables, ρ, p and T (the temperature) are related by the equation of state so that only two are independent, and with the use of equation of state the equation of the fifth row (i.e., the equation of energy) can be expressed in terms of temperature (see, for example, Kneer and Nakagawa, 1976).

The set of Eqs. (6)–(13) is of the form

$$a_{rpq}\frac{\partial w_q}{\partial x_r} + s_p = 0 \tag{14}$$

where w_q $(q = 1, 2, \ldots, 8)$ are physical variables, a_{rpq} and s_p $(p = 1, 2, \ldots, 8)$ are functions of w_q and x_r, and x_r $(r = 1, 2, 3, 4)$ are the independent variables; hereafter x_1 is specified as the time variable and x_2, x_3, x_4 are spatial coordinates.

A surface ϕ can be defined in the x_r-space by

$$\phi(x_1, x_2, x_3, x_4) = 0\,. \tag{15}$$

Let us introduce a set of new coordinates $\sigma_1, \sigma_2, \sigma_3, \sigma_4$, which are chosen such that $\sigma_2, \sigma_3, \sigma_4$ determine a position on the surface ϕ while $\sigma_1 = \phi$. In terms of these new coordinates, Eq. (14) can be written in the form

$$a_{rpq}\frac{\partial \sigma_1}{\partial x_r}\frac{\partial w_q}{\partial \sigma_1} + \left(a_{rpq}\frac{\partial \sigma_i}{\partial x_r}\frac{\partial w_q}{\partial \sigma_i}\right)_{i \geq 2} + s_p = 0\,, \tag{16}$$

with the use of the formula of transformation of derivatives,

$$\frac{\partial w_q}{\partial x_r} = \frac{\partial \sigma_i}{\partial x_r}\frac{\partial w_q}{\partial \sigma_i}\,.$$

Equation (16) can be solved for $\partial w_q/\partial \sigma_1$ provided that the matrix $a_{rpq}(\partial \sigma_1/\partial x_r)$ has an inverse. Conversely, if the determinant composed of $a_{rpq}(\partial \sigma_1/\partial x_r)$ is zero, the normal derivatives to the surface $\sigma_1 = \phi$ are indeterminate. This is the condition of defining the characteristic surface ϕ in the multi-dimensional and multi-variable problems, i.e.,

$$\det\left|a_{rpq}\frac{\partial \phi}{\partial x_r}\right| = 0\,, \tag{17}$$

where we write σ_1 in terms of ϕ as $\sigma_1 = \phi$. Then a set of linear coefficients λ_p to be found satisfying

$$\lambda_p a_{rpq}\frac{\partial \phi}{\partial x_r} = 0\,,$$

and the resultant equation after multiplying λ_p to Eq. (16) less the first term is called the compatibility equations for the characteristic surface $\phi = \text{const}$ (Sauerwein, 1966).

Physically, the definition of the characteristic surface by Eq. (17) is equivalent to find a surface in the (t, x, y, z)-space across which physical variables can have arbitrary jumps. This can be understood by considering the difference of Eq. (16) written at point P^+ and P^- on either side of the surface ϕ and let the point P^+ and P^- approach arbitrarily close to a point P on ϕ. Then the derivative along the surface ϕ as well as s_p will cancel each other out and only the first term will remain. Under such circumstances, if Eq. (17) is satisfied, arbitrary jumps of w_q across the surface ϕ are possible as we can write (Jeffrey and Taniuti, 1964);

$$\frac{\partial w_q}{\partial \phi} \propto [w_q(P^+) - w_q(P^-)]\,.$$

For the present problem, it has been shown by Sauerwein (1966) and Nakagawa (1980) after solving Eq. (17) that the characteristic surfaces are given by

$$\frac{D\phi}{Dt} = 0, \tag{18a}$$

$$\left(\frac{D\phi}{Dt}\right)^2 - (\boldsymbol{b} \cdot \nabla\phi)^2 = 0, \tag{18b}$$

$$\left(\frac{D\phi}{Dt}\right)^2 - C_f^2 = 0, \tag{18c}$$

$$\left(\frac{D\phi}{Dt}\right)^2 - C_s^2 = 0, \tag{18d}$$

where

$$\boldsymbol{b} = \boldsymbol{B}/\sqrt{\rho} \tag{18e}$$

$$C_f^2 = \tfrac{1}{2}|\nabla\phi|\left[|\nabla\phi|(a^2+b^2) + \{(\nabla\phi)^2(a^2+b^2)^2 - 4a^2(\boldsymbol{b}\cdot\nabla\phi)^2\}^{1/2}\right] \tag{18f}$$

$$C_s^2 = \tfrac{1}{2}|\nabla\phi|\left[|\nabla\phi|(a^2+b^2) - \{(\nabla\phi)^2(a^2+b^2) - 4a^2(\boldsymbol{b}\cdot\nabla\phi)^2\}^{1/2}\right] \tag{18g}$$

and $(\boldsymbol{b}, \nabla\phi)$, c_f and c_s denote the transverse, fast and slow MHD wave speeds in the direction of $\nabla\phi$.

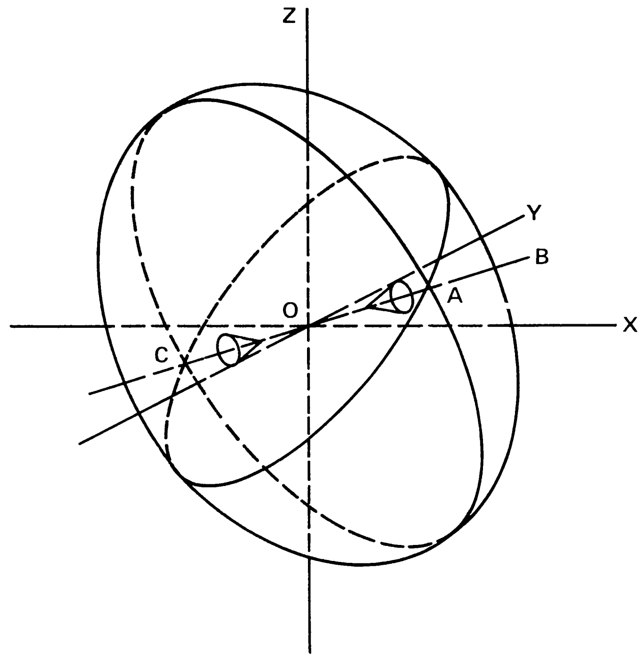

Fig. 1. The loci of MHD wave fronts due to a point source disturbance moving with the fluid velocity at O. OB denotes the direction of magnetic field. The ellipsoidal surface represents the loci of fast wave fronts, two triangular cones are the loci of slow wave fronts, and the points A and C are the loci of transverse wave fronts

2.3. *Physical identification of characteristic surfaces*

Normal to the surfaces given by Eqs. (18a–d) finite jumps of physical variables are possible. Thus let us proceed with their physical identifications, starting with Eq. (18a)

$$\frac{D\phi}{Dt} = \frac{\partial\phi}{\partial t} + u\frac{\partial\phi}{\partial x} + v\frac{\partial\phi}{\partial y} + w\frac{\partial\phi}{\partial z} = 0$$

If we compare this expression with the directional derivative of the function ϕ along a curve $s(t, x, y, z)$ in the x_r-space, i.e.,

$$\frac{d\phi}{ds} = \frac{\partial\phi}{\partial t}\frac{\partial t}{\partial s} + \frac{\partial\phi}{\partial x}\frac{\partial x}{\partial s} + \frac{\partial\phi}{\partial y}\frac{\partial y}{\partial s} + \frac{\partial\phi}{\partial z}\frac{\partial z}{\partial s},$$

it is evident that the curve $s(t, x, y, z)$ is the fluid (particle) trajectory, since integration yields that the surface ϕ is characterized by the direction cosines which are identical to the velocity components

$$\frac{dx}{dt} = u, \quad \frac{dy}{dt} = v, \quad \frac{dz}{dt} = w.$$

The discontinuity normal to such a surface ϕ = const is the contact discontinuity (i.e., the piston surface). Thus the characteristic surface given by Eq. (18a) can be identified with the trajectory of the contact discontinuity. In a similar manner, the other characteristic surfaces can be identified with the trajectories, respectively, the loci of transverse (Alfven) wave fronts for Eq. (18b), loci of the fast wave fronts for Eq. (18c) and loci of the slow wave fronts for Eq. (18d). In Eqs. (18b–d), all the terms are expressed as squares which imply that these loci can propagate with time both in the positive and negative directions of the (x, y, z) coordinates, also the presence of the factor $D\phi/Dt$ implies that these propagations are relative to the particle trajectory, i.e., the fluid motion.

The typical geometrical properties of these loci relative to the fluid motion are illustrated in Fig. 1, in which the fluid is assumed to be at rest and the direction of magnetic field is taken as OB direction. The ellipsoidal surface symmetric around the OB axis is the loci of fast wave fronts, two circular cones also symmetric around the OB axis are the loci of slow wave fronts and the points A and C along the axis OB are the loci of transverse wave fronts. With the lapse of time these loci propagate in the (x, y, z)-space, and it can be noticed that volume changes result only for the loci fast and slow waves, thus the formation of shocks are limited to these waves.

2.4. *Method of projected characteristics*

Apart from the contact discontinuity, the compatibility equations are exceedingly complex (see, for example, Sauerwein, 1966). This results from the difficulties in finding a set of linear coefficients λ_p and the coordinates $\sigma_2, \sigma_3, \sigma_4$ in terms of analytical functions of x_r, and complex numerical procedures must be employed. The method of projected characteristics is designed to abbreviate this complexity by writing the compatibility equations in the component (x, t), (y, t) and (z, t) planes. The first successful attempt of this approach was reported by Shih and Kot (1978) for two dimensional hydrodynamic problems as the alternative to the method of characteristics when the method of characteristics became too cumbersome or outright impossible.

Expressing the different spatial derivatives separately, Eqs. (6)–(13) can be rewritten in the following matrix form

$$\frac{\partial \boldsymbol{w}}{\partial t} = -\left(\boldsymbol{A}\frac{\partial}{\partial x} + \boldsymbol{B}\frac{\partial}{\partial y} + \boldsymbol{C}\frac{\partial}{\partial z}\right)\boldsymbol{W} + \boldsymbol{S}, \tag{19}$$

where $\boldsymbol{W}$ and $\boldsymbol{S}$ are column vectors, and $\boldsymbol{A}$ and $\boldsymbol{B}$ and $\boldsymbol{C}$ are 8×8 matrices, identical to those given in Nakagawa (1981a) except for the change of coordinate systems (cartesian here, spherical there).

$$W = \begin{vmatrix} \rho \\ u \\ v \\ w \\ p \\ B_x \\ B_y \\ B_z \end{vmatrix}, \quad S = \begin{vmatrix} 0 \\ 0 \\ 0 \\ -g \\ (\gamma - 1)\Delta Q \\ 0 \\ 0 \\ 0 \end{vmatrix}, \tag{20}$$

Then for the derivation of compatibility equations, say, in the (x, t) plane, we write Eq. (19) in the form,

$$\frac{\partial \boldsymbol{W}}{\partial t} + \boldsymbol{A}\frac{\partial \boldsymbol{W}}{\partial x} = -\left(\boldsymbol{B}\frac{\partial \boldsymbol{W}}{\partial y} + \boldsymbol{C}\frac{\partial W}{\partial z}\right) + \boldsymbol{S}. \tag{21}$$

Next we look for the characteristic curves in the (x, t) plane and this is achieved by finding the eigenvalues of α of the matrix A, i.e., through the equation,

$$\mathrm{dot}\,|\boldsymbol{A} - \alpha \boldsymbol{I}| = 0, \tag{22}$$

where $\boldsymbol{I}$ is the unit matrix.

Specifically from Eq. (22), eight eigenvalues are obtained

$$\alpha^{(1)} = u,\ \alpha^{(2)} = u,\ \alpha^{(3)} = u + U_A,\ \alpha^{(4)} = u - U_A,$$
$$\alpha^{(5)} = u + U_f,\ \alpha^{(6)} = u - U_f,\ \alpha^{(7)} = u + U_s,\ \alpha^{(8)} = u - U_s, \tag{23}$$

where

$$U_A = \left|\frac{B_x}{\sqrt{\rho}}\right| = |b_x|$$

$$U_f^2 = \frac{1}{2}\{a^2 + b^2 + [(a^2 + b^2)^2 - 4a^2 b_x^2]^{1/2}\}, \tag{24}$$

$$U_s^2 = \frac{1}{2}\{a^2 + b^2 - [(a^2 + b^2)^2 - 4a^2 b_x^2]^{1/2}\}.$$

The eigenvalues u and $\pm U_A$ correspond exactly to the projections of the loci of the characteristic surfaces given by Eqs. (18a–b) to the x axis while $\pm U_f$ and $\pm U_s$ correspond to the points of intersections of the x axis with the planes tangential to the loci of fast and slow wave fronts and normal to the x axis, as shown in Figs. 2 and 3.

With the characteristic directions given by the eigenvalues $\alpha^{(j)}$ ($j = 1, 2, \ldots, 8$), the next procedure of finding a set of linear coeffi-

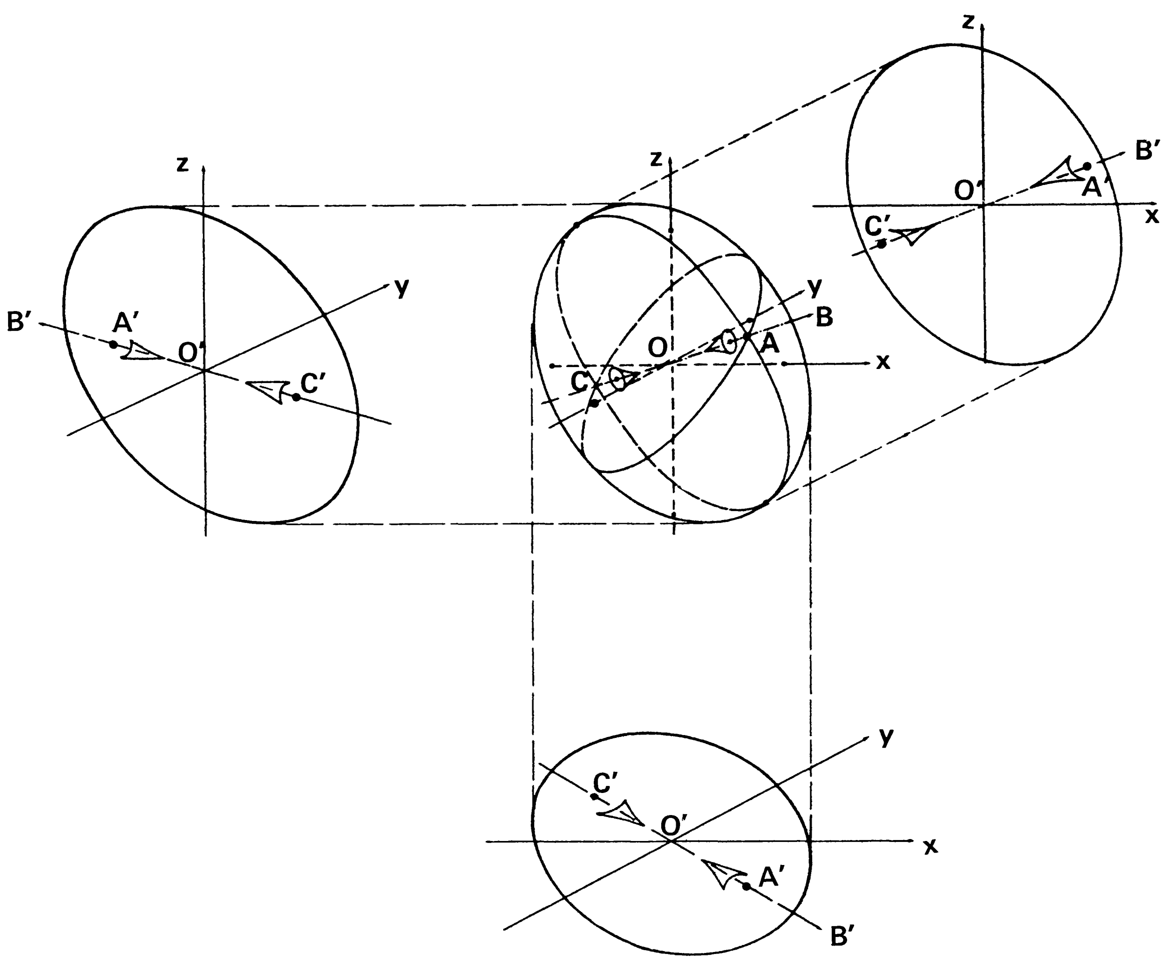

Fig. 2. The relationship between three- and two-dimensional loci of characteristic surfaces. The direction of magnetic field in the (x, y, z)-coordinates is represented by OB and the projections are denoted by O'B'. A' and C' are the projections of A and C, i.e., the wave fronts of transverse (Alfven) waves

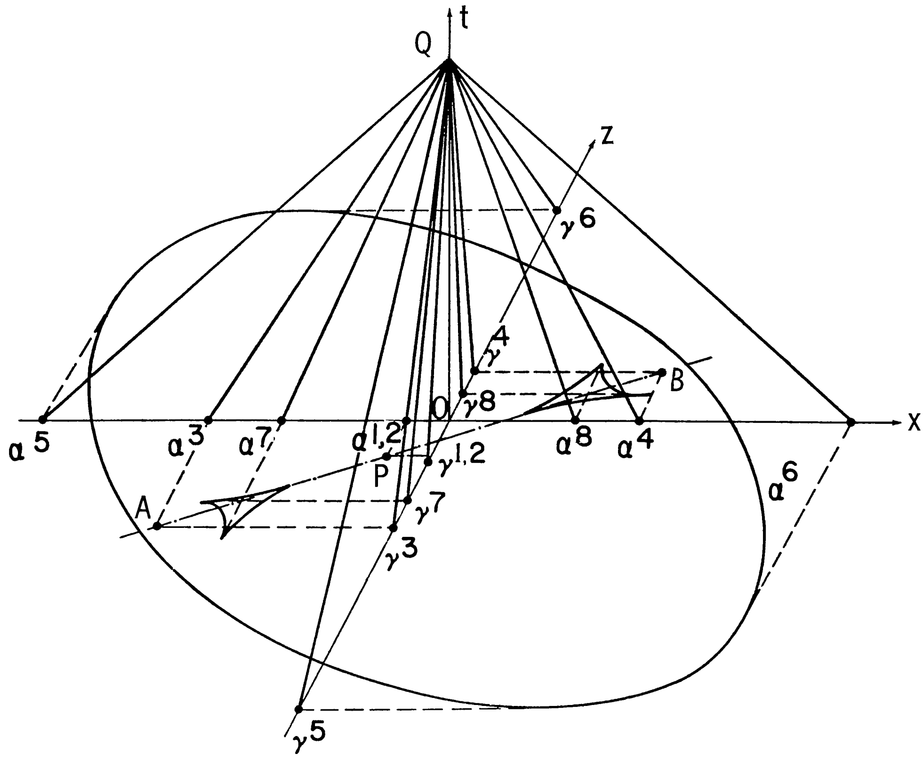

Fig. 3. The loci of characteristics and foot-points of projected characteristics. α^j and γ^j ($j = 1, 2, \ldots, 8$) denote the foot-points and APB is the direction of magnetic field. Note that the foot-points are determined by the interactions of planes tangential to the loci and normal to the x or z axis

cients for the derivation of compatibility equations along these characteristics, is replaced by finding the left-eigenvectors $\xi^{(j)}$ associated with each of the eigenvalues from the equation,

$$\xi^{(j)} A = \alpha^{(i)} \xi^{(j)} \tag{25}$$

In this determination one of the eight components of each eigenvector remains arbitrary, however, this represents a common factor and does not affect subsequent results.

The compatibility equation in the (x, t) plane is obtained by scalar multiplication of $\xi^{(j)}$ to Eq. (21), with the use of Eq. (25), in the form

$$\xi^{(j)}\left(\frac{\partial W}{\partial t} + A\frac{\partial W}{\partial x}\right) = -\xi^{(j)}\left(B\frac{\partial W}{\partial y} + C\frac{\partial W}{\partial z}\right) + \xi^{(j)} S$$

or

$$\xi^{(j)}\frac{dW}{ds^{(j)}} = -\xi^{(j)}\left(B\frac{\partial W}{\partial y} + C\frac{\partial W}{\partial z}\right) + \xi^{(j)} S, \tag{26}$$

as the left hand side can be transformed

$$\xi^{(j)}\left(\frac{\partial W}{\partial t} + A\frac{\partial W}{\partial x}\right) = \xi^{(j)}\left(\frac{\partial W}{\partial t} + \alpha^{(j)}\frac{\partial W}{\partial x}\right) = \xi^{(j)}\frac{dW}{ds^{(j)}},$$

where the direction of the characteristic curve $s^{(j)}\,(x, t)$ is

$$\frac{dx}{dt} = \alpha^{(j)}. \tag{27}$$

Equation (26) is similar to Eq. (2) in the form, thus by integrating Eq. (26) along the curve $s^{(j)}$, eight integral relations of the form of Eq. (5) can be obtained and from these integral relations the eight physical variables can be determined uniquely. This is the basic approach of the method of projected characteristics, and repeating such determinations in each of the (x, t), the (y, t) and (z, t) planes independently then take the average for the final result.

The discrepancy arising from this procedure of the method of projected characteristics and the genuine method of characteristics is the difference of the domain of dependence for the determination of the change of variables due to projection effect. Furthermore, a considerable mathematical manipulation is involved in deriving the compatibility equations in the genuine method of characteristics (see, for example, Sauerwein, 1966), both methods could lead to the similar accuracy as demonstrated by Shin and Kot (1978). Therefore, the major advantage of the present method is that the physical causality relationships can be readily identified for each of eight projected characteristics and subsequently enable us to derive the physical proper boundary equations in a systematic manner as described in Sect. 4.

3. Basic formulations

In the practical application, the determination of the change of physical variables are performed numerically in each of the component planes, after rewriting Eq. (26) in the form of difference equations, while approximating the characteristic curves by straight lines. First, in each of the component planes, the directions of projected characteristics are determined by the equations,

$$\det|A - \alpha I| = 0, \quad \det|B - \beta I| = 0, \quad \det|C - \gamma I| = 0, \tag{28}$$

where α, β, and γ are the eigenvalues for the matrices $\boldsymbol{A}$, $\boldsymbol{B}$ and $\boldsymbol{C}$, respectively. Associated with each of the eight eigenvalues, $\alpha^{(j)}$, $\beta^{(j)}$ and $\gamma^{(j)}$ $(j = 1, 2, \ldots, 8)$, the left-eigenvectors are found in the (x, t), (y, t) and (z, t) planes from equations,

$$\xi^{(j)}\boldsymbol{A} = \alpha^{(j)}\xi^{(j)}, \quad \boldsymbol{\eta}^{(j)}\boldsymbol{B} = \beta^{(j)}\boldsymbol{\eta}^{(j)}, \quad \zeta^{(j)}\boldsymbol{C} = \gamma^{(j)}\zeta^{(j)} \tag{29}$$

where $\xi^{(j)}$, $\boldsymbol{\eta}^{(j)}$ and $\zeta^{(j)}$ $(j = 1, 2, \ldots, 8)$ denote the left-eigenvectors in each of the component planes.

Then the compatibility equations along each projected characteristic are obtained in the following forms, i.e., along $dx/dt = \alpha^{(j)}$.

$$\xi^{(j)}\frac{\partial \boldsymbol{W}}{\partial t} = -\xi^{(j)}\left(\alpha^{(j)}\frac{\partial}{\partial x} + \boldsymbol{B}\frac{\partial}{\partial y} + \boldsymbol{C}\frac{\partial}{\partial z}\right)\boldsymbol{W} + \xi^{(j)}\boldsymbol{S}, \tag{30a}$$

and along $dy/dt = \beta^{(j)}$

$$\boldsymbol{\eta}^{(j)}\frac{\partial \boldsymbol{W}}{\partial t} = -\boldsymbol{\eta}^{(j)}\left(\boldsymbol{A}\frac{\partial}{\partial x} + \beta^{(j)}\frac{\partial}{\partial y}\boldsymbol{C}\frac{\partial}{\partial z}\right)\boldsymbol{W} + \boldsymbol{\eta}^{(j)}\boldsymbol{S}, \tag{30b}$$

and along $dz/dt = \gamma^{(j)}$

$$\zeta^{(j)}\frac{\partial \boldsymbol{W}}{\partial t} = -\zeta^{(j)}\left(\boldsymbol{A}\frac{\partial}{\partial x} + \boldsymbol{B}\frac{\partial}{\partial y} + \gamma^{(j)}\frac{\partial}{\partial z}\right)\boldsymbol{W} + \zeta^{(j)}\boldsymbol{S}, \tag{30c}$$

where the column vectorial nature of Eqs. (30a–c) is understood. The compatibility equations obtained in this manner can be expressed in a table identical to Table 1 in Nakagawa (1981a) where the right-hand sides (R.H.S.) of Eqs. (30a–c) are expressed as α_j, β_j and γ_j $(j = 1, 2, \ldots, 8)$ for abbreviation, and new notations are:

$$\begin{aligned}
&V_A = |b_y|, \quad W_A = |b_z|, \\
&V_f^2 = \tfrac{1}{2}\{a^2 + b^2 + [(a^2+b^2)^2 - 4a^2b_y^2]^{1/2}\}, \\
&V_s^2 = \tfrac{1}{2}\{a^2 + b^2 - [(a^2+b^2)^2 - 4a^2b_y^2]^{1/2}\}, \\
&W_f^2 = \tfrac{1}{2}\{a^2 + b^2 + [(a^2+b^2)^2 - 4a^2b_z^2]^{1/2}\}, \\
&W_s^2 = \tfrac{1}{2}\{a^2 + b^2 - [(a^2+b^2)^2 - 4a^2b_z^2]^{1/2}\},
\end{aligned} \tag{31}$$

with b_x, b_y and b_z denoting the components of the Alfven velocity, i.e.,

$$b_x = \frac{B_x}{\sqrt{\rho}}, \quad b_y = \frac{B_y}{\sqrt{\rho}}, \quad b_z = \frac{B_z}{\sqrt{\rho}}, \quad b^2 = b_x^2 + b_y^2 + b_z^2 .$$

It should be noted that a, b, U_f, U_s, V_f, V_s, W_f and W_s always represent positive quantities, while b_x, b_y and b_z can change sign depending upon the signs of B_x, B_y and B_z.

In such a table (see Nakagawa, 1981a), the specific eigenvalues are listed in the first column and the components of the left-eigenvectors associated with each eigenvalue are given in the second to eighth columns; the last column lists the quantities on the right-hand sides (R.H.S.) of Eqs. (30a–c). This table will not be repeated here. Thus the compatibility equation along a specific projected characteristic can be obtained by equating the terms in the row. For example, in the (x, t) plane, along the projected characteristic $dx/dt = u + U_A$, the compatibility equation is

$$-b_yb_z(\partial v/\partial t) + b_xb_y(\partial w/\partial t) + b_zU_A(\partial B_y/\partial t) - b_yU_A(\partial B_z/\partial t) = \alpha_3,$$

where α_3 is the sum of terms on the right-hand side of equations, of $\partial v/\partial t$ multiplied by $-b_yb_z$, $\partial w/\partial t$ by b_xb_y, $\partial B_y/\partial t$ by $b_zU_A/\sqrt{\rho}$ and $\partial B_z/\partial t$ by $-b_yU_A/\sqrt{\rho}$. Thus it is evident that eight equations are obtained for eight physical variables of $\boldsymbol{W}$ in each of the (x, t), (y, t) and (z, t) planes, and these equations can be solved as a set of simultaneous algebraic equations to determine the eight temporal variations $\partial \boldsymbol{W}/\partial t$ uniquely in each of the projected planes.

In practice, before determining the temporal variations $\partial \boldsymbol{W}/\partial t$, we write each compatibility equation in the difference form following the rule described in the Appendix A taking into account of the direction of each projected characteristic. Then for the final determination of $\partial \boldsymbol{W}/\partial t$ is achieved by taking the average of such directional results of $\partial \boldsymbol{W}/\partial t$. These procedures lead, after some algebraic manipulations, to the final equation for the determination of $\partial \boldsymbol{W}/\partial t$ in the following difference form for the three dimensional problem,

$$\begin{aligned}\Delta_t\boldsymbol{W} = &-\boldsymbol{A}(\Delta_x\boldsymbol{W}) - \boldsymbol{B}(\Delta_y\boldsymbol{W}) - \boldsymbol{C}(\Delta_z\boldsymbol{W}) + \boldsymbol{S} \\ &+ \boldsymbol{D}(\delta_x\boldsymbol{W}) + \boldsymbol{E}(\delta_y\boldsymbol{W}) + \boldsymbol{F}(\delta_z\boldsymbol{W}).\end{aligned} \tag{32}$$

Here in reference to a time step $p\,\Delta t$ and a grid point (l, m, n), the quantity $\Delta_t\boldsymbol{W}$ is

$$\Delta_t\boldsymbol{W}^p_{l,m,n} = \frac{\boldsymbol{W}^{p+1}_{l,m,n} - \boldsymbol{W}^{*p}_{l,m,n}}{\Delta t}, \tag{33a}$$

with

$$\begin{aligned}\boldsymbol{W}^{*p}_{l,m,n} = \tfrac{1}{6}(&\boldsymbol{W}^p_{l+1,m,n} + \boldsymbol{W}^p_{l-1,m,n} + \boldsymbol{W}^p_{l,m+1,n} + \boldsymbol{W}^p_{l,m-1,n} \\ &+ \boldsymbol{W}^p_{l,m,n+1} + \boldsymbol{W}^p_{l,m,n-1})\end{aligned}$$

and typical spatial derivatives are, say in the x direction,

$$\begin{aligned}\Delta_x\boldsymbol{W}^p_{l,m,n} &= \frac{\boldsymbol{W}^p_{1+l,m,n} - \boldsymbol{W}^p_{l-1,m,n}}{2\Delta x}, \\ \delta_x\boldsymbol{W}_{l,m,n} &= \frac{\boldsymbol{W}^p_{l+1,m,n} - 2\boldsymbol{W}^p_{l,m,n} + \boldsymbol{W}^p_{l-1,m,n}}{2\Delta x}.\end{aligned} \tag{33b}$$

The similar definitions in the y and z directions are understood. The quantities denoted by $\boldsymbol{D}$, $\boldsymbol{E}$ and $\boldsymbol{F}$ are 8×8 matrices, identical to those given in Nakagawa (1981a).

The common factor $\frac{1}{3}$ appearing in the matrices $\boldsymbol{D}$, $\boldsymbol{E}$ and $\boldsymbol{F}$ denotes the consequence of averaging for the three component planes, i.e., (x, t), (y, t) and (z, t) planes, as each of these matrices are uniquely determined in each of the component planes through the algebraic procedure described in the Appendix A. Physically, Eq. (32) shows that the variation of physical variables at a given location and time is the sum of variations, namely, the variation resulting from temporal extrapolation of original equation (the terms associated with $\boldsymbol{A}$, $\boldsymbol{B}$, $\boldsymbol{C}$ and $\boldsymbol{S}$) and the variation due to the terms associated with the matrices $\boldsymbol{D}$, $\boldsymbol{E}$ and $\boldsymbol{F}$. The latter can be identified with the variation communicated through the characteristics. In fact, dimensionally the term with $\delta\boldsymbol{W}$ denotes flux, thus these terms can be considered as corrections to simple temporal extrapolation.

4. Examination of numerical stability

In the strict sense, the numerical stability for nonlinear difference equations remains empirical. However, for practical purposes, it is preferable to satisfy the criterion of stability at least for the linearized version of Eq. (32). For simplicity, let $\Delta x = \Delta y = \Delta z$;

then by expressing $\boldsymbol{W}^p_{l,m,n}$ in terms of $\boldsymbol{W}^p_0 \exp(ik_x l\,\Delta x + ik_y m\,\Delta x + ik_z n\,\Delta x)$ (where, $\boldsymbol{W}^p_0$ is a constant vector for each time step p), we can define the amplification matrix $\boldsymbol{G}$ by writing Eq. (32) in the form (Richtmayer and Moreton, 1976),

$$\boldsymbol{W}^{p+1}_0 = \boldsymbol{G}\boldsymbol{W}^p_0 \tag{34}$$

with

$$\boldsymbol{G} = \tfrac{1}{3}(\cos\alpha^* + \cos\beta^* + \cos\gamma^*)\boldsymbol{I} - i(\boldsymbol{A}\sin\alpha^* + \boldsymbol{B}\sin\beta^* + \boldsymbol{C}\sin\gamma^*)\left(\frac{\Delta t}{\Delta t}\right) + [\boldsymbol{D}(\cos\alpha^* - 1) + \boldsymbol{E}(\cos\beta^* - 1) + \boldsymbol{F}(\cos\gamma^* - 1)]\left(\frac{\Delta t}{\Delta x}\right) \tag{35}$$

where $\alpha^* = k_x\,\Delta x$, $\beta^* = k_y\,\Delta x$ and $\gamma^* = k_z\,\Delta x$.

The numerical stability is satisfied, if the largest eigenvalue of the matrix $\boldsymbol{G}$ is less than unity. It should be noted that in this linear stability analysis, the matrices $\boldsymbol{A}$, $\boldsymbol{B}$, $\boldsymbol{C}$, $\boldsymbol{D}$, $\boldsymbol{E}$ and $\boldsymbol{F}$ are considered constant, while the term $\boldsymbol{S}$ is dropped as this term can be reduced to null with $\Delta t \to 0$. The matrix $\boldsymbol{G}$ is complex; however, $\boldsymbol{G}$ can be made symmetric by multiplication of ρ to the second, third and fourth rows and division by $a^2\rho$ of the fifth row. Nevertheless, the determination of the eigenvalues of the matrix $\boldsymbol{G}$ remains a rather complicated mathematical task. Hence, let $\beta^* = \gamma^* = 0$ to gain some insight; then we find that the elements G_{11} and G_{66} yield the following eigenvalues:

$$\lambda_1 = \lambda_2 = \frac{\cos\alpha^* + 2}{3} - i\left(\frac{\Delta t}{\Delta x}\right)u\sin\alpha^*. \tag{36}$$

This implies for stability

$$|\lambda_{1,2}| = \left(\frac{\cos\alpha^* + 2}{3}\right)^2 - \epsilon^2\sin^2\alpha^* \le 1, \tag{37}$$

where $\epsilon = u(\Delta t/\Delta x)$. Considering $|\lambda_{1,2}|^2$ as a function of α^*, the angle α^* at which $|\lambda_{1,2}|^2$ attains the maximum value is found to be

$$\alpha^* = 0, \quad \pi \text{ and } \cos^{-1}\left(\frac{2}{9\epsilon^2 - 1}\right). \tag{38}$$

The angle $\cos^{-1}(2/9\epsilon^2 - 1)$ appears to provide the only physically meaningful result, and with this value $|\lambda_{1,2}|^2$ becomes

$$|\lambda_{1,2}|^2 = \frac{3}{(9\epsilon^2 - 1)^2}[12\epsilon^4 + (9\epsilon^2 + 1)(3\epsilon^2 - 1)]. \tag{39}$$

The extremum of $|\lambda_{1,2}|^2$ is then found to be associated with

$$\epsilon = \frac{\sqrt{3}}{3}. \tag{40}$$

However, the value of $\epsilon > \sqrt{3}/3$ yields $|\lambda_{1,2}|^2 > 1$. Therefore, for the stability, the requirement becomes

$$\epsilon \le \frac{\sqrt{3}}{3}, \quad \text{i.e., } \Delta t \le \frac{\sqrt{3}}{3}\frac{\Delta x}{u}. \tag{41}$$

It can be checked with $\epsilon = \sqrt{3}/3$; the maximum possible value of $|\lambda_{1,2}|^2$ is unity for $\alpha^* = 0$.

For the remaining elements, the maximum eigenvalue can be found by dropping the terms containing u (i.e., by setting $u = 0$) in comparison with those containing U_f, U_A and U_s. Then the matrix $\boldsymbol{G}$ can be reduced to the following form,

$$\begin{vmatrix} G'_{22} & -B_xB_yY & -B_xB_zY & -iZ & -iB_yZ & -iB_zZ \\ -B_xB_yY & G'_{33} & G'_{34} & 0 & iB_xZ & 0 \\ -B_xB_zY & G'_{43} & G'_{44} & 0 & 0 & +iB_xZ \\ -iZ & 0 & 0 & G'_{55} & \dfrac{B_y}{\rho}Y & \dfrac{B_z}{\rho}Y \\ -iB_yZ & iB_xZ & 0 & \dfrac{B_y}{\rho}Y & G'_{79} & G'_{78} \\ -iB_zZ & 0 & iB_xZ & \dfrac{B_z}{\rho}Y & G'_{87} & G'_{88} \end{vmatrix} \tag{42}$$

where

$$\begin{aligned}
G'_{22} &= \rho\{G'_{11} + [a(a + U_A) + b_y^2 + b_z^2]Y\},\\
G'_{33} &= \rho\left\{G'_{11} + \frac{U_A[b_y^2(a + U_A) + b_z^2(U_f + U_s)]}{b_y^2 + b_z^2}Y\right\},\\
G'_{34} &= G'_{43} = \frac{B_yB_zU_A(a + U_A - U_f - U_s)}{b_y^2 + b_z^2}Y,\\
G'_{44} &= \rho\left\{G'_{11} + \frac{U_A[b_y^2(U_f + U_s) + b_z^2(a + U_A)]}{b_y^2 + b_z^2}Y\right\},\\
G'_{55} &= \frac{1}{a^2\rho}\{G'_{11} + a(a + U_A)Y\},\\
G'_{77} &= G'_{11} + \frac{b_y^2(aU_A + b^2) + b_z^2U_A(U_f + U_s)}{b_y^2 + b_z^2}Y,\\
G'_{78} &= G'_{87} = \frac{b_yb_z[aU_A + b^2 - U_A(U_f + U_s)]}{b_y^2 + b_z^2}Y,\\
G'_{88} &= G'_{11} + \frac{b_y^2U_A(U_f + U_s) + b_z^2(aU_A + b^2)}{b_y^2 + b_z^2}Y,
\end{aligned} \tag{43}$$

with

$$G'_{11} = \frac{\cos\alpha^* + 2}{3}, \quad Y = \left(\frac{\Delta t}{\Delta x}\right)\frac{\cos\alpha^* - 1}{3(U_f + U_s)}, \quad Z = \left(\frac{\Delta t}{\Delta x}\right)\sin\alpha^*. \tag{44}$$

After some mathematical manipulation, the eigenvalues of Eq. (42) are found to satisfy

$$\begin{aligned}
&\left\{\left[G'_{11} - \lambda - U_f\left(\frac{\Delta t}{\Delta x}\right)\frac{(1 - \cos\alpha^*)}{3}\right]^2 + \left[U_f\left(\frac{\Delta t}{\Delta x}\right)\sin\alpha^*\right]^2\right\}\\
&\times\left\{\left[G'_{11} - \lambda - U_s\left(\frac{\Delta t}{\Delta x}\right)\frac{(1 - \cos\alpha^*)}{3}\right]^2 + \left[U_s\left(\frac{\Delta t}{\Delta x}\right)\sin\alpha^*\right]^2\right\}\\
&\times\left\{\left[G'_{11} - \lambda - U_A\left(\frac{\Delta t}{\Delta x}\right)\frac{(1 - \cos\alpha^*)}{3}\right]^2 + \left[U_A\left(\frac{\Delta t}{\Delta x}\right)\sin\alpha^*\right]^2\right\} = 0,
\end{aligned} \tag{45}$$

so that the eigenvalues are

$$\lambda_{3,4} = \frac{\cos\alpha^* + 2}{3} - \left[U_f \frac{(1-\cos\alpha^*)}{3} \pm iU_f \sin\alpha^*\right]\left(\frac{\Delta t}{\Delta x}\right),$$
$$\lambda_{5,6} = \frac{\cos\alpha^* + 2}{3} - \left[U_s \frac{(1-\cos\alpha^*)}{3} \pm iU_s \sin\alpha^*\right]\left(\frac{\Delta t}{\Delta x}\right), \quad (46)$$
$$\lambda_{7,8} = \frac{\cos\alpha^* + 2}{3} - \left[U_A \frac{(1-\cos\alpha^*)}{3} \pm iU_A \sin\alpha^*\right]\left(\frac{\Delta t}{\Delta x}\right).$$

With $U_f > U_A > U_s$, clearly the largest eigenvalues are given by $\lambda_{3,4}$. Therefore, the stability is given by

$$|\lambda_{3,4}|^2 = \left[\frac{\cos\alpha^* + 2}{3} - \frac{\epsilon^*(1-\cos\alpha^*)}{3}\right]^2 + \epsilon^{*2}\sin^2\alpha^* \le 1 \quad (47)$$

where $\epsilon^* = U_f(\Delta t/\Delta x)$. Again, looking for the angle α^* at which $|\lambda_{3,4}|^2$ attains the maximum value, we obtain

$$\alpha^* = 0, \quad \pi \text{ and } \cos^{-1}\left[\frac{(1+\epsilon^*)(2-\epsilon^*)}{(4\epsilon^*+1)(2\epsilon^*-1)}\right]. \quad (48)$$

Hence, by setting

$$\cos^{-1}\left[\frac{(1+\epsilon^*)(2-\epsilon^*)}{(4\epsilon^*+1)(2\epsilon^*-1)}\right] = 1, \quad (49)$$

the extremum of $|\lambda_{3,4}|^2$ is found to be associated with

$$\epsilon^* \ge \frac{1+\sqrt{13}}{6}. \quad (50)$$

However, this condition again leads to $|\lambda_{3,4}|^2 > 1$; hence the stability condition becomes

$$\Delta t < \frac{1+\sqrt{13}}{6}\frac{\Delta x}{U_f}. \quad (51)$$

With $U_f \gg u$, the condition Eq. (51) overrides the condition Eq. (41). Note that with $\epsilon^* = 1 + \sqrt{13}/6$, $|\lambda_{3,4}|^2 = 1$ for $\alpha^* = 0$.

Now restoring u into the above manipulation, we find that the eigenvalues given in Eq. (46) are modified by replacements of U_f by $U_f \pm u$, U_s by $U_s \pm u$ and U_A by $U_A \pm u$. In other words, the criterion Eq. (51) holds with U_f replaced by $(|u| + |U_f|)$. Accordingly, for the general case, we conclude that the following criterion secures the linear numerical stability.

$$\Delta t < \frac{1+\sqrt{13}}{6}\frac{\Delta x}{v^*} \quad (52)$$

with

$$v^* = [(|u| + |U_f|)^2 + (|v| + |V_f|)^2 + (|w| + |W_f|)^2]^{1/2}.$$

5. Derivation of boundary equations

The hyperbolic nature of basic equations requires that the change of physical variables on the boundary surface must be treated as the initial-boundary value problem as mentioned previously. Thus when the time-dependent changes are given for a certain set of variables on the boundary surface, the changes of unspecified variables must be found to satisfy the compatibility equations. In addition, depending upon the physical circumstances, some projected characteristics can lie outside of the domain of computation and lose their physical significance. Therefore, a proper choice must be made to obtain the appropriate boundary equations. For simplicity, with the assumption of two-dimensionality ($\partial/\partial y = 0$), the derivation of boundary equations appropriate to the study of the evolution of magnetic arches due to motions of their foot-points is described. The general physical circumstances of the problem is illustrated in Fig. 4. The plane $z = 0$ is considered as a surface of constant pressure and density on which the motion of foot-points is prescribed. The motion of foot-points is further assumed to be anti-symmetric with respect to the plane $x = 0$ and its x-directional motion to vanish at $x = \pm x_0$.

The assumption of two-dimensionality ($\partial/\partial y = 0$) leads to the following modifications of the formulae given in Sects. 3 and 4.

(1) All the coefficients associated with $\partial/\partial y$ to vanish, so that the matrices $\boldsymbol{B}$ and $\boldsymbol{E}$ are null, also one of the spatial indexes.

(2) The dimensional factor $\frac{1}{3}$ for the matrices $\boldsymbol{D}$ and $\boldsymbol{F}$ to be replaced by $\frac{1}{2}$, also the factor $\frac{1}{6}$ for $\boldsymbol{W}^*p$ by $\frac{1}{4}$.

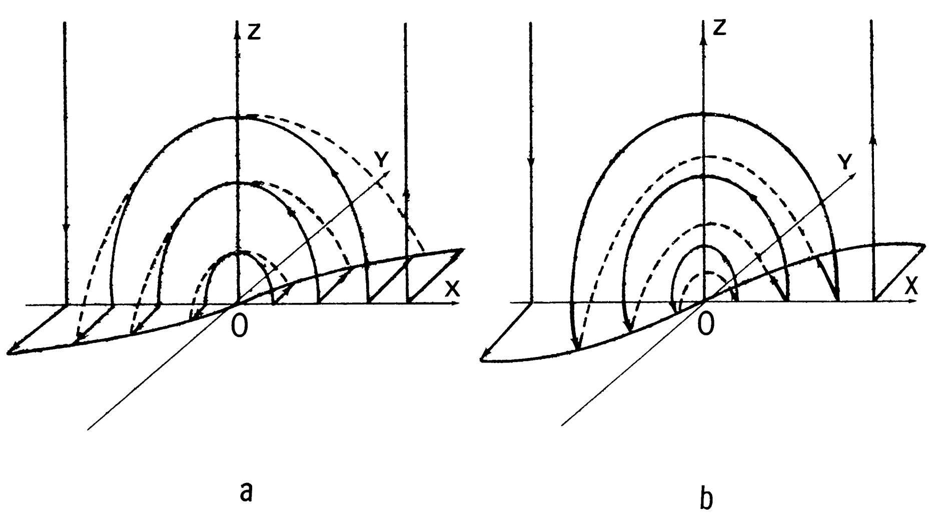

Fig. 4. A schematic illustration of physical situation for the evolution of two-dimensional dipole subject to a pure lateral shearing motion, **a**, and a more general motion, **b**, of the magnetic foot-points

(3) The time step of Δt for the numerical stability in Eq. (52) to be replaced by

$$\Delta t < \frac{\Delta x}{2v'}, \quad \Delta t < \frac{\Delta z}{2v'}, \qquad (53)$$
$$v' = [(|u| + |U_f|)^2 + |v|^2 + (|w| + |W_f|)^2]^{1/2}.$$

In addition, some of the physical properties and their temporal variations are prescribed on the boundary surface; those specifications of physical variables change the matrices $\boldsymbol{A}$ and $\boldsymbol{C}$ on the boundary surface to $\boldsymbol{A}^*$ and $\boldsymbol{C}^*$ (hereafter the asterisk is used to denote values on the boundary surface whenever needed). This change of matrices to $\boldsymbol{A}^*$ and $\boldsymbol{C}^*$ leads to the change of eigenvalues to $\alpha^{*(j)}$ and $\gamma^{*(j)}$, also the subsequent change of left-eigenvectors to $\xi^{*(j)}$ and $\zeta^{*(j)}$.

The final consequence of these changes is the modification of the compatibility equations. Further, the presence of the boundary surface limits the number of physically meaningful projected characteristics to those intersecting the boundary surface from the domain of computation. These modifications necessitate the derivation of specific boundary equations on each specific boundary surface as given below.

5.1. *The boundary surface* $x = 0$.

The condition of evolution remaining anti-symmetric with respect to the plane $x = 0$, yields, with geometrical considerations,

$$u = \frac{\partial u}{\partial z} = \frac{\partial u}{\partial t} = 0, \qquad v = \frac{\partial v}{\partial z} = \frac{\partial v}{\partial t} = 0,$$
$$B_z = \frac{\partial B_z}{\partial z} = \frac{\partial B_z}{\partial t} = 0, \quad \frac{\partial w}{\partial x} = \frac{\partial B_x}{\partial x} = \frac{\partial B_y}{\partial x} = 0, \quad \text{for } x = 0. \qquad (54)$$

The conditions $\partial v/\partial t = 0$ and $\partial B_z/\partial t = 0$ are satisfied automatically. However, the requirement of $\partial u/\partial t = 0$ leads to the following additional conditions for self-consistency,

$$\frac{\partial \rho}{\partial x} = \frac{\partial p}{\partial x} = 0, \quad \text{for } x = 0. \qquad (55)$$

In other words, five boundary equations become necessary for the determination of $\partial\rho/\partial t$, $\partial w/\partial t$, $\partial p/\partial t$, $\partial B_x/\partial t$, $\partial B_y/\partial t$ on the plane $x = 0$. The needed sets of compatibility equations along physically meaningful projected characteristics are summarized in Table 1. These sets are obtained from the inspection of Fig. 5 showing the loci of characteristics and the locations of foot-points of the physically meaningful projected characteristics in the (x, z)-plane. It may be noted that from the table the compatibility equation along a specific projected characteristic can be obtained by equating the terms on the same row. For example, along $dx/dt = u - U_f$, the compatibility equation is $(U_f^2 - b_x^2/\rho)(\partial p/\partial t) - (U_f^2 b_y/\sqrt{\rho})(\partial B_y/\partial t) = \alpha_4^*$, where α_4^* denotes the sum of the terms on the right-hand sides (R.H.S.) of $\partial p/\partial t$ multiplied by $(U_f^2 - b_x^2/\rho)$ and $\partial B_y/\partial t$ by $(U_f^2 b_y/\sqrt{\rho})$ adjusted by

Table 1. Compatibility equations on the plane $x = 0$

Eigenvalues	$\frac{\partial\rho}{\partial t}$	$\frac{\partial w}{\partial t}$	$\frac{1}{\rho}\frac{\partial p}{\partial t}$	$\frac{1}{\sqrt{\rho}}\frac{\partial B_x}{\partial t}$	$\frac{1}{\sqrt{\rho}}\frac{\partial B_y}{\partial t}$	R.H.S.
$\frac{dx}{dt} = 0$	a^2		$-\rho$			α_1^*
$\frac{dx}{dt} = 0$				1		α_2^*
$\frac{dx}{dt} = u - U_A$		1				α_3^*
$\frac{dx}{dt} = u - U_f$			$U_f^2 - b_x^2$		$b_y U_f^2$	α_4^*
$\frac{dx}{dt} = u - U_s$			$b_x^2 - U_s^2$		$-b_y U_s^2$	α_5^*
$\frac{dz}{dt} = w$	a^2		$-\rho$			β_1^*
$\frac{dz}{dt} = w$				b_y	$-b_x$	β_2^*
$\frac{dz}{dt} = w$			$b_x^2 + b_y^2$	$a^2 b_x$	$-a^2 b_y$	β_3^*
$\frac{dz}{dt} = w + W_f$		W_f	1	b_x	b_y	β_4^*
$\frac{dz}{dt} = w - W_f$		$-W_f$	1	b_x	b_y	β_5^*

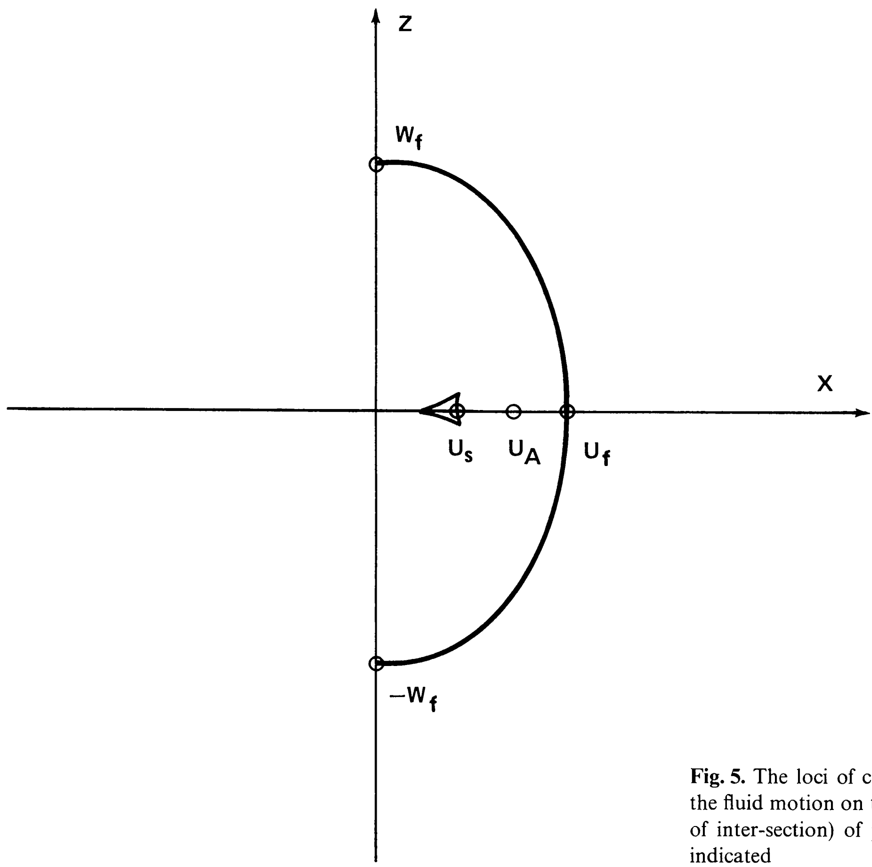

Fig. 5. The loci of characteristics and characteristic surfaces relative to the fluid motion on the (x, z)-plane for $x = 0$. The foot-points (the points of inter-section) of physically meaningful projected characteristics are indicated

the conditions given in Eqs. (54) and (55). Note that with $B_z = 0$, $W_A = W_s = 0$.

After writing the compatibility equations in the different forms following the rule described in the Appendix B, the compatibility equations are solved as sets of simultaneous algebraic equations for temporal variations of the unspecified physical variables in the (x, t) and (z, t) planes independently. Then the boundary equations are obtained by taking the average of these independent determinations to compensate the directional effects. The boundary equations thus obtained are (suppressing the asterisk)

$$\Delta_t \rho = R_\rho(\Delta_x^+ \boldsymbol{W}, \Delta_z \boldsymbol{W}) + \frac{\rho w}{2W_f}(\delta_z w) + \frac{1}{2W_f}(\delta_z p) + \frac{B_x}{2W_f}(\delta_z B_x) + \frac{B_y}{2W_f}(\delta_z B_y), \tag{56a}$$

$$\Delta_t w = R_w(\Delta_x^+ \boldsymbol{W}, \Delta_z \boldsymbol{W}) + \frac{W_f}{2}(\delta_z w) + \frac{w}{2\rho W_f}(\delta_z p) + \frac{B_x w}{2\rho W_f}(\delta_z B_x) + \frac{B_y w}{2\rho W_f}(\delta_z B_y), \tag{56b}$$

$$\Delta_t p = R_p(\Delta_x^+ \boldsymbol{W}, \Delta_z \boldsymbol{W}) + \frac{\rho a^2 w}{2W_f}(\delta_z w) + \frac{a^2}{2W_f}(\delta_z p) + \frac{a^2 B_x}{2W_f}(\delta_z B_x) + \frac{a^2 B_y}{2W_f}(\delta_z B_y), \tag{56c}$$

$$\Delta_t B_x = R_{B_x}(\Delta_x^+ \boldsymbol{W}, \Delta_z \boldsymbol{W}) + \frac{B_x w}{2W_f}(\delta_z w) + \frac{B_x}{2\rho W_f}(\delta_z p) + \frac{b_x^2}{2W_f}(\delta_z B_x) + \frac{b_x b_y}{2W_f}(\delta_z B_y), \tag{56d}$$

$$\Delta_t B_y = R_{B_y}(\Delta_x^+ \boldsymbol{W}, \Delta_z \boldsymbol{W}) + \frac{B_y w}{2W_f}(\delta_z w) + \frac{B_y}{2\rho W_f}(\delta_z p) + \frac{b_x b_y}{2W_f}(\delta_z B_x) + \frac{b_y^2}{2W_f}(\delta_z B_y). \tag{56e}$$

Here $\Delta_t \boldsymbol{W}$ denotes the quantity defined in the Appendix B and the new notation; for example, $R_\rho(\Delta_x^+ \boldsymbol{W}, \Delta_z \boldsymbol{W})$ represents the right-hand side of the ρ-component of Eq. (1) modified by the prescribed conditions, and the derivative $\partial \boldsymbol{W}/\partial x$ and $\partial \boldsymbol{W}/\partial z$ expressed by $\Delta_x^+ \boldsymbol{W}$ and $\Delta_z \boldsymbol{W}$ defined in the Appendix B.

5.2. The boundary surface $z = 0$.

On the surface $z = 0$, the prescribed conditions are

$$u = u_G(x, t), \qquad v = v_G(x, t), \qquad \frac{\partial \rho}{\partial x} = \frac{\partial p}{\partial x} = 0, \qquad \frac{\partial \rho}{\partial t} = \frac{\partial p}{\partial t} = 0, \tag{57}$$

where the quantities with the subscript G represent the physical properties prescribed as functions of x and t. With Eq. (57) four boundary equations are required for $\partial w/\partial t$, $\partial B_x/\partial t$, $\partial B_y/\partial t$ and $\partial B_z/\partial t$. Then from Fig. 6, the needed compatibility equations are found as summarized in Table 2. After some algebraic manipulations, the boundary equations are obtained as follows.

$$
\begin{aligned}
\Delta_t w = {} & R_w(\Delta_x \boldsymbol{W}, \Delta_z^+ \boldsymbol{W}) - \frac{2b_x b_z + a(W_A - U_A + a)}{2(a + W_A)W_A}\left(\frac{\Delta u}{\Delta t}\right) \\
& - \frac{b_y(a + 2W_A)}{2b_z(a + W_A)}\left(\frac{\Delta v}{\Delta t}\right) \\
& + \frac{W_A(W_f + W_s) + (a + W_A)(U_f - U_s)}{2\rho a(a + W_A)W_A}\left(\frac{\Delta p}{\Delta t}\right) \\
& + \frac{a(a^2 + b^2 - 2b_x^2) - (a + U_A)(U_f - U_s)u}{2(U_t + U_s)W_A}(\delta_x u) \\
& - \frac{b_x b_y[2aU_A + (U_f - U_s)u]}{2U_A W_A(U_f + U_s)}(\delta_x v) \\
& + \frac{2aU_A + (U_f - U_s)u}{2(U_f + U_s)}(\delta_x w) - \frac{aB_y(U_f - U_s - 2u)}{2\rho(U_f + U_s)W_A}(\delta_x B_y) \\
& - \frac{aB_z(U_f - U_s - 2u)}{2\rho(U_f + U_s)W_A}(\delta_x B_z),
\end{aligned}
\tag{58a}
$$

$$
\begin{aligned}
\Delta_t B_x = {} & R_{B_x}(\Delta_x \boldsymbol{W}, \Delta_z^+ \boldsymbol{W}) - \frac{B_z[b_x^2(W_f + W_s) + b_y^2(a + W_A)]}{2(b_x^2 + b_y^2)(a + W_A)W_A}\left(\frac{\Delta u}{\Delta t}\right) \\
& + \frac{B_y U_A(W_f + W_s - W_A - a)}{2(b_x^2 + b_y^2)(a + W_A)}\left(\frac{\Delta v}{\Delta t}\right) + \frac{B_x}{2\rho(a + W_A)}\left(\frac{\Delta p}{\Delta t}\right)
\end{aligned}
\tag{58b}
$$

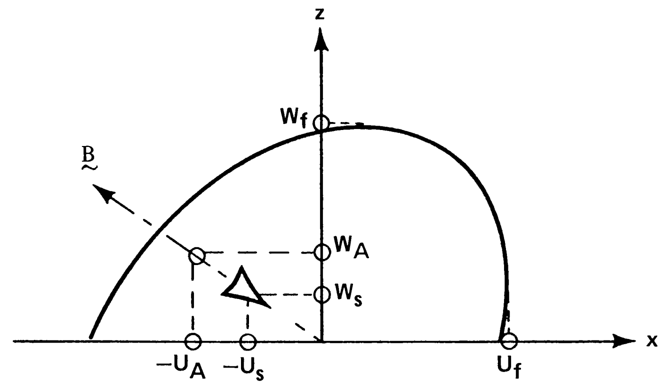

Fig. 6. The loci of characteristics and characteristic surfaces relative to the fluid motion on the (x, z)-plane for $z = 0$. The foot-points of physically meaningful projected characteristics are indicated and B refers to the projected direction of the magnetic field

$$
\begin{aligned}
\Delta_t B_y = {} & R_{B_y}(\Delta_x \boldsymbol{W}, \Delta_z^+ \boldsymbol{W}) + G_1\left(\frac{\Delta u}{\Delta t}\right) + G_2\left(\frac{\Delta v}{\Delta t}\right) + G_3\left(\frac{\Delta p}{\Delta t}\right) \\
& + D_1^*(\delta_x u) + D_2^*(\delta_x v) + D_3^*(\delta_x w) + D_4^*(\delta_x B_y) + D_5^*(\delta_x B_z),
\end{aligned}
\tag{58c}
$$

$$
\begin{aligned}
\Delta_t B_z = {} & R_{B_z}(\Delta_x \boldsymbol{W}, \Delta_z^+ \boldsymbol{W}) + G_4\left(\frac{\Delta u}{\Delta t}\right) + \frac{B_y}{2W_A}\left(\frac{\Delta v}{\Delta t}\right) + G_5\left(\frac{\Delta p}{\Delta t}\right) \\
& + D_6^*(\delta_x U) + D_7^*(\delta_x v) + D_8^*(\delta_x w) + D_9^*(\delta_x B_y) + D_{10}^*(\delta_x B_y),
\end{aligned}
\tag{58d}
$$

Table 2. Compatibility equations on the plane $z = 0$

Eigenvalue	$\frac{\partial w}{\partial t}$	$\frac{1}{\sqrt{\rho}}\frac{\partial B_x}{\partial t}$	$\frac{1}{\sqrt{\rho}}\frac{\partial B_y}{\partial t}$	$\frac{1}{\sqrt{\rho}}\frac{\partial B_z}{\partial t}$	R.H.S.
$\frac{dx}{dt} = u$		1			α_1^*
$\frac{dx}{dt} = u + U_A$	$-b_x b_y$		$-b_z U_A$	$b_y U_A$	$\alpha_2^* - b_x b_z\left(\frac{\Delta v}{\Delta t}\right)$
$\frac{dx}{dt} = u - U_f$	$b_x b_z U_f$		$b_y U_f^2$	$b_z U_f^2$	$\alpha_3^* + U_f(U_f^2 - b_x^2)\left(\frac{\Delta u}{\Delta t}\right) - b_x b_y U_f\left(\frac{\Delta v}{\Delta t}\right) - (U_f^2 - b_x^2)\left(\frac{1}{\rho}\frac{\Delta p}{\Delta t}\right)$
$\frac{dx}{dt} = u + U_s$	$b_x b_z U_s$		$-b_y U_s^2$	$-b_z U_s^2$	$\alpha_4^* - U_s(b_x^2 - U_s^2)\left(\frac{\Delta u}{\Delta t}\right) - b_x b_y U_s\left(\frac{\Delta v}{\Delta t}\right) - (b_x^2 - U_s^2)\left(\frac{1}{\rho}\frac{\Delta p}{\Delta t}\right)$
$\frac{dz}{dt} = w$				1	β_1^*
$\frac{dz}{dt} = w - W_A$		$b_y W_A$	$b_x W_A$		$\beta_2^* - b_y b_z\left(\frac{\Delta u}{\Delta t}\right) + b_x b_z\left(\frac{\Delta v}{\Delta t}\right)$
$\frac{dz}{dt} = w - W_f$	$-W_f(W_f^2 - b_z^2)$	$b_x W_f^2$	$b_y W_f^2$		$\beta_3^* - b_x b_z W_f\left(\frac{\Delta u}{\Delta t}\right) - b_y b_z W_f\left(\frac{\Delta v}{\Delta t}\right) - (W_f^2 - b_z^2)\left(\frac{1}{\rho}\frac{\Delta p}{\Delta t}\right)$
$\frac{dz}{dt} = w - W_s$	$-W_s(b_z^2 - W_s^2)$	$-b_x W_s^2$	$-b_y W_s^2$		$\beta_4^* + b_x b_z W_s\left(\frac{\Delta u}{\Delta t}\right) + b_y b_z W_s\left(\frac{\Delta v}{\Delta t}\right) - (b_z^2 - W_s^2)\left(\frac{1}{\rho}\frac{\Delta p}{\Delta t}\right)$

where

$$G_1 = B_y[(b_x^2 + b_y^2)(U_f - U_s + U_A - a)(a + W_A) + (b_y^2 + b_z^2)U_A(W_f + W_s - W_A - a)]/ 2(b_x^2 + b_y^2)(b_y^2 + b_z^2)(a + W_A),$$

$$G_2 = -B_z[2b_x^2(a + W_A) + b_y^2(W_f + W_s + W_A + a)]/ 2(b_x^2 + b_y^2)(a + W_A)W_A,$$

$$G_3 = B_y[b_y^2 + b_z^2 + (a + W_A)(U_f - U_s + U_A - a)]/ 2\rho a(b_y^2 + b_z^2)(a + W_A),$$

$$G_4 = B_x[b_y^2(U_A - a) - b_z^2(U_f - U_s)]/2(b_y^2 + b_z^2)U_A W_A,$$

$$G_5 = B_x[b_y^2(U_f - U_s) - b_z^2(U_A - a)]/2\rho a(b_y^2 + b_z^2)U_A W_A,$$

$$D_1^* = B_y\{a(a^2 + b^2 - 2b_x^2) - [a(a + U_A) + (b_y^2 + b_z^2)](U_f - U_s) + [a^2 + b^2 - 2b_x^2 - (a + U_A)(U_f - U_s)]u\}/ 2(b_y^2 + b_z^2)(U_f + U_s),$$

$$D_2^* = B_x\{[b_y^2(U_f - U_s - 2a) - b_z^2(U_f + U_s)]U_A - [b_y^2(U_f - U_s + 2U_A) + b_z^2(U_f + U_s)]u\}/ 2(b_y^2 + b_z^2)U_A(U_f + U_s),$$

$$D_3^* = -B_y[U_A(U_f - a) - (U_A - U_s)u]W_A/(b_y^2 + b_z^2)(U_f + U_s),$$

$$D_4^* = \{b_y^2[a^2 + b^2 - a(U_f + U_s)] + b_z^2U_A(U_f + U_s) - [b_y^2(U_f - U_s - 2a) - b_z^2(U_f + U_s)]u\}/ 2(b_y^2 + b_z^2)(U_f + U_s),$$

$$D_5^* = b_y b_z[a^2 + b^2 - a(U_f - U_s) - U_A(U_f + U_s) - 2(U_f - a)u]/2(b_y^2 + b_z^2)(U_f + U_s),$$

$$D_6^* = B_x\{ab_y^2(a^2 + b^2 - 2b_x^2) + b_z^2[a(a + U_A) + b_y^2 + b_z^2](U_f - U_s) - [b_y^2(a + U_A)(U_f - U_s) + b_z^2(a^2 + b^2 - 2b_x^2)]u\}/ 2(b_y^2 + b_z^2)U_A(U_f + U_s)W_A,$$

$$D_7^* = -B_y\{2U_A(ab_y^2 + b_z^2U_f) + [b_y^2(U_f - U_s) + b_z^2(U_f + U_s - 2U_A)]u\}/2(b_y^2 + b_z^2)(U_f + U_s)W_A,$$

$$D_8^* = -B_x\{U_A[b_y^2(U_f + U_s - 2a) - b_z^2(U_f - U_s)] + 2(b_y^2U_s + b_z^2U_A u\}/2(b_y^2 + b_z^2)U_A(U_f + U_s),$$

$$D_9^* = -b_x b_y\{ab_y^2(U_f - U_s) + b_z^2[a^2 + b^2 - U_A(U_f + U_s)] - 2(ab_y^2 + b_z^2U_f)u\}/2(b_y^2 + b_z^2)U_A(U_f + U_s)W_A,$$

$$D_{10}^* = \{b_y^2[a(U_f - U_s) + U_A(U_f + U_s)] + b_z^2(a_2 + b_2) + [b_y^2(U_f + U_s - 2a) - b_z^2(U_f - U_s)]u\}/2(b_y^2 + b_z^2)(U_f + U_s). \tag{59}$$

The new notation in Eqs. (58a–d) is

$$\left(\frac{\Delta W}{\Delta t}\right) = \left(\frac{\partial W}{\partial t}\right)_G - R_W(\Delta_x W, \Delta_z^+ W) \tag{60}$$

which represents the net effect of prescribed boundary condition $(\partial W/\partial t)_G$ on the unspecified variables. In traditional analysis, this term is set equal to zero and the compatibility equations are derived from the remaining unspecified variables. However, under general circumstances, the prescribed $(\partial W/\partial t)_G$ is not necessarily compatible with the terms on the right-hand side, i.e., $R_W(\Delta_x W, \Delta_z^+ W)$. Therefore, dropping this term from the boundary equations is equivalent to ignoring the general compatibility conditions governing all physical variables. In other words, this term is needed to retain physical self-consistency of the analysis and to secure the continuity and smoothness of the solutions on the boundary surfaces. This is a fundamental contribution of the present method to the analysis of initial-boundary value problems.

5.3. The boundary surface $x = x_0$.

The definition of $x = x_0$ as the magnetic pole with vanishing velocity u, yields with geometrical considerations,

$$u = \frac{\partial u}{\partial z} = \frac{\partial u}{\partial t} = 0, \quad B_x = \frac{\partial B_x}{\partial z} = \frac{\partial B_x}{\partial t} = 0,$$

$$\frac{\partial \rho}{\partial x} = \frac{\partial p}{\partial x} = \frac{\partial B_z}{\partial x} = 0. \tag{61}$$

Thus, six boundary equations are required for $\partial\rho/\partial t$, $\partial v/\partial t$, $\partial w/\partial t$, $\partial p/\partial t$, $\partial B_y/\partial t$ and $\partial B_z/\partial t$. The compatibility equations for the determination of the above quantities are summarized in Table 3 on the basis of Fig. 7. Note that with $B_x = 0$, $b_x = U_A = U_s = 0$ in this case. The boundary equations obtained from these compatibility equations are:

$$\Delta_t \rho = R_\rho(\Delta_x^- W, \Delta_z W) + \frac{\rho b_y b_z w}{2aW_W(W_f + W_s)}(\delta_z v) + \frac{\rho(a + W_A)w}{2a(W_f + W_s)}(\delta_z w) + \frac{a + W_A}{2a(W_f + W_s)}(\delta_z p) + \frac{B_y}{2(W_f + W_s)}(\delta_z B_y) \tag{62a}$$

$$\Delta_t v = R_v(\Delta_x^- W, \Delta_z W) + \frac{(a + W_A)W_A}{2(W_f + W_s)}(\delta_z v) - \frac{b_y b_z}{2(W_f + W_s)}(\delta_z w) + \frac{b_y b_z w}{2\rho a W_A(W_f + W_s)}(\delta_z p) - \frac{B_z(a + W_A)w}{2\rho W_A(W_f + W_s)}(\delta_z B_y), \tag{62b}$$

$$\Delta_t w = R_w(\Delta_x^- W, \Delta_z W) - \frac{b_y b_z}{2(W_f + W_s)}(\delta_z v) + \frac{a(a + W_A) + b_y^2}{2(W_f + W_s)}(\delta_z w) + \frac{(a + W_A)w}{2\rho a(W_f + W_s)}(\delta_z p) + \frac{B_y w}{2\rho(W_f + W_s)}(\delta_u B_y), \tag{62c}$$

$$\Delta_t p = R_p(\Delta_x^- W, \Delta_z W) + \frac{\rho a b_y b_z w}{2W_A(W_f + W_s)}(\delta_z v) + \frac{\rho a(a + W_A)w}{2(W_f + W_s)}(\delta_z w) + \frac{a(a + W_A)}{2(W_f + W_s)}(\delta_z p) + \frac{a^2 B_y}{2(W_f + W_s)}(\delta_z B_y), \tag{62d}$$

$$\Delta_t B_y = R_{B_y}(\Delta_x^- W, \Delta_z W) - \frac{B_z(a + W_A)w}{2W_A(W_f + W_s)}(\delta_z v) + \frac{B_y w}{2(W_f + W_s)}(\delta_z w) + \frac{B_y}{2\rho(W_f + W_s)}(\delta_z p) + \frac{aW_A + b_y^2 + b_z^2}{2(W_f + W_s)}(\delta_z B_y), \tag{62e}$$

$$\Delta_t B_z = R_{B_z}(\Delta_x^- W, \Delta_z W). \tag{62f}$$

Table 3. Compatibility equations on the plane $x = x_0$

Eigenvalue	$\frac{\partial \rho}{\partial t}$	$\frac{\partial v}{\partial t}$	$\frac{\partial w}{\partial t}$	$\frac{1}{\rho}\frac{\partial p}{\partial t}$	$\frac{1}{\sqrt{\rho}}\frac{\partial B_y}{\partial t}$	$\frac{1}{\sqrt{\rho}}\frac{\partial B_z}{\partial t}$	R.H.S.
$\frac{dx}{dt} = 0$	a^2			$-\rho$			α_1^*
$\frac{dx}{dt} = 0$		1					α_2^*
$\frac{dx}{dt} = 0$			1				α_3^*
$\frac{dx}{dt} = 0$					b_z	$-b_y$	α_4^*
$\frac{dx}{dt} = 0$				$b_y^2 + b_z^2$	$-a^2 b_y$	$-a^2 b_z$	α_5^*
$\frac{dx}{dt} = U_f$				1	b_y	b_z	α_6^*
$\frac{dz}{dt} = w$	a^2			$-\rho$			β_1^*
$\frac{dz}{dt} = w$						1	β_2^*
$\frac{dz}{dt} = w + W_f$		$-b_y b_z W_f$	$W_f(W_f^2 - b_z^2)$	$W_f^2 - b_z^2$	$b_y W_f^2$		β_3^*
$\frac{dz}{dt} = w - W_f$		$b_y b_z W_f$	$-W_f(W_f^2 - b_z^2)$	$W_f^2 - b_z^2$	$b_y W_f^2$		β_4^*
$\frac{dz}{dt} = w + W_s$		$b_y b_z W_s$	$W_s(b_z^2 - W_s^2)$	$b_z^2 - W_s^2$	$-b_y W_s^2$		β_5^*
$\frac{dz}{dt} = w - W_s$		$-b_y b_z W_s$	$-W_s(b_z^2 - W_s^2)$	$b_z^2 - W_s^2$	$-b_y W_s^2$		β_6^*

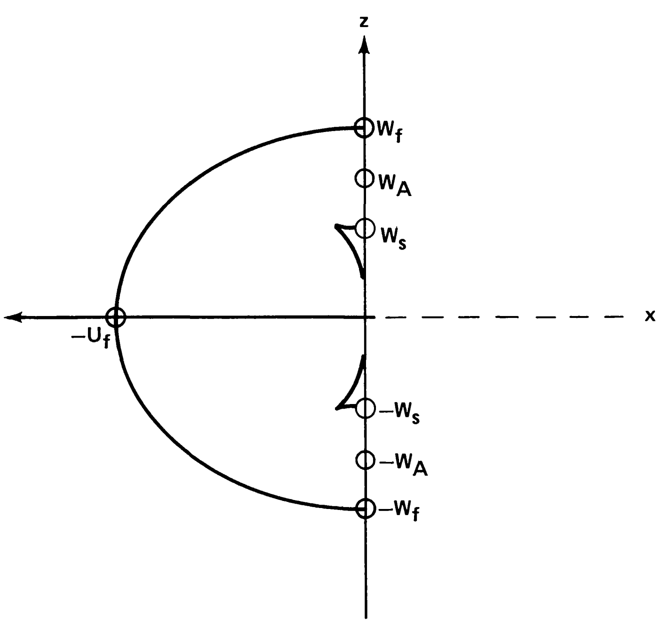

Fig. 7. The loci of characteristics and characteristic surfaces relative to the fluid motion on the (x, z)-plane for $x = x_0$. The foot-points of physically meaningful projected characteristics are indicated

It may be noted that the coefficients associated with $\delta_z \boldsymbol{W}$ are similar to those given by $\boldsymbol{F}$ with $b_x = 0$, as almost all the compatibility equations in the (z, t)-plane are available for the determination of temporal variations of unspecified physical quantities.

5.4. The boundary surface $z = z_0$.

The top boundary $z = z_0$ is an artificial boundary; therefore, apart from the limitation imposed on the z-direction derivatives with respect to the domain analysis, the boundary equations remain identical with the equations determining the temporal variation of W within the domain of analysis. In other words, the boundary equation is given by

$$\Delta_t \boldsymbol{W} = -\boldsymbol{A}(\Delta_x \boldsymbol{W}) - \boldsymbol{C}(\Delta_z^+ \boldsymbol{W}) + \boldsymbol{S} + \boldsymbol{D}(\delta_z \boldsymbol{W}), \tag{63}$$

with the spatial and temporal derivatives denoting the quantities defined in the Appendix B.

6. Numerical examples

These formulations have been applied to practical problems of evolution of atmospheric magnetic field of the Sun. Two specific types of motions at $z = 0$ level are considered; case (i) a purely

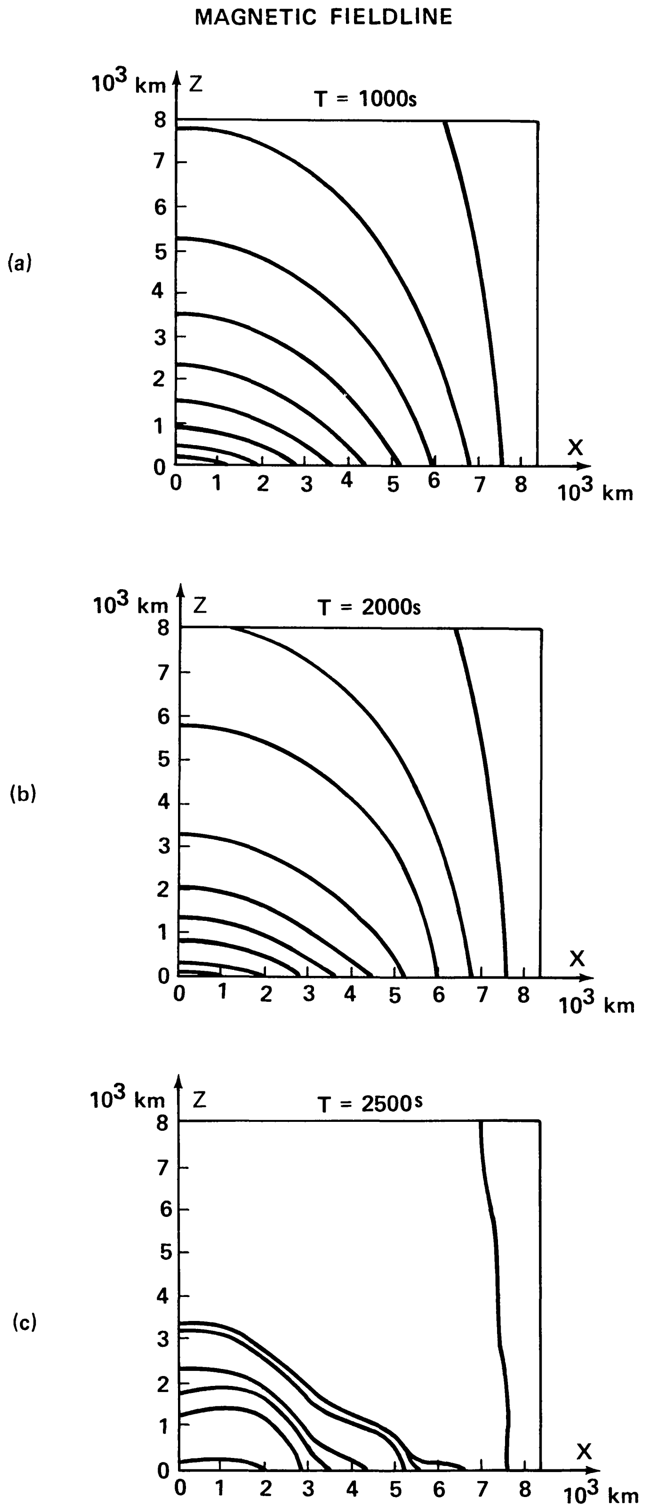

Fig. 8. The computed evolution of magnetic arches due to a shearing motion of their foot-points. T refers to the lapse time in sec. for the maximum velocity of shear 2 $\mathrm{km\,s^{-1}}$

shearing motion characterized by $u = u_G(x, t) = 0$ and $v = v_G(x, t)$, and case (ii) purely diverging and converging motions confined in the (x, z) plane so that $u = u_G(x, t)$ and $v = 0$. In these studies, the evolution of physical variables on the boundary surfaces are evaluated according to the boundary equations in Sect. 5. In Fig. 8, the result of evolution of the atmospheric magnetic field due to a shearing motion of foot-points is illustrated and in Fig. 9 the similar result due to a diverging motion is shown.

In these computations it is found that the boundary equations derived in the manner described in Sect. 5 and the Appendix B provide stable and physically self-consistent boundary changes of the variables.

7. Discussion and concluding remarks

The formulation of the projected characteristics clearly show that any variation of physical quantity for a given spatial location and time can be identified with the consequence of finite amplitude disturbances arriving from the domain of dependence. Further, it is shown that the present formulation can provide a systematic and physically self-consistent means of analyzing megnetohydrodynamic nonlinear initial-boundary value problems. For the evolution of magnetic arches due to their foot-points motion, some preliminary results were obtained which showed that the general atmospheric response is the accumulation of mass toward the center of the arches. However, their subsequent evolution was found to depend strongly on the initial as well as boundary conditions. For example, for a strong initial magnetic field, the evolved field configuration approaches those of non-constant α force-free field given by Low (1977).

In contrast, with a weak initial magnetic field, the evolution is strongly governed by the gravitational effect on the accumulated mass and subsequent deformation of magnetic field; the latter could be correlated with the possible onset of current driven instability of plasma in lower layers of atmosphere. The details of each specific problem is beyond the scope of the present paper, nevertheless, some remarks on the present formulation can be made as follows.

Clearly the present formulation provides the means of physically realistic understanding of complex nonlinear magneto-hydrodynamic problems of astro-physics. For example, the formation of multi-dimensional shocks and particular consequence of the specific physical effect as the latter effect can be traced by the following particular characteristic or projected characteristics. In addition, the present formulation provides physical insight for the derivation of the proper boundary equations according to different physical circumstances. For example, the number of available compatibility equations on the boundary surface can be determined by counting the number of projected characteristics intersecting the boundary surface for a given physical circumstance from the computational domain. Hence, the number of physical variables and their temporal variations to be specified are readily known. In particular, such information is extremely important in treating free-boundary problems in which flows can freely cross the boundary surface. It is hoped that further use of this formulation to various types of astrophysical problems will lead to more refinement of this approach.

Acknowledgement. This work was supported by a NASA Grant (NAGW-9), NASA/MSFC Grant (NAG8-053) and NASA MSFC Contract (NAS 833526) and Air Force Contract F19628-82-K-0014.

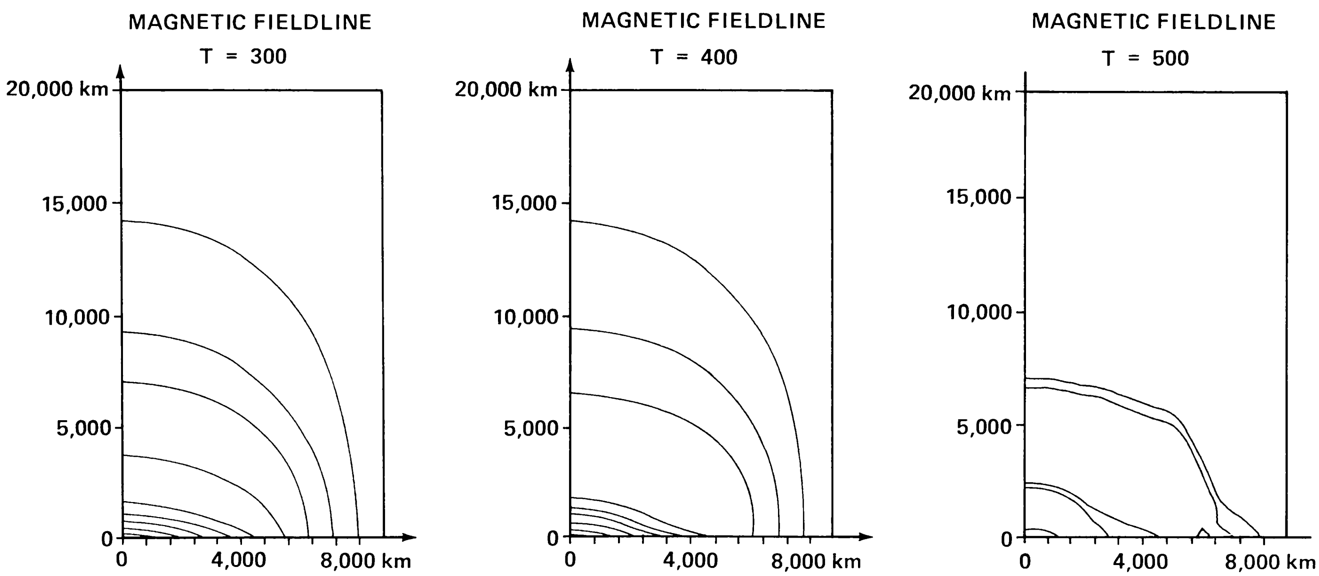

Fig. 9. The computed evolution of magnetic arches due to a diverging motion from the $x = 0$ axis (a purely two dimensional computational results in the (x, z)-plane). T refers to the lapse time in sec. and the maximum velocity of divergence is taken as $2\,\mathrm{km\,s^{-1}}$

Appendix A

In deriving the difference form of the compatibility equations in the projected planes, a certain rule is applied for expressing the spatial derivatives. As an example, let us consider the (x, t) plane, then for a small time difference Δt the projected characteristics given by

$$\frac{dx}{dt} = \alpha^{(j)} \quad (j = 1, 2, \ldots, 8) \tag{A.1}$$

can be approximated by straight lines as shown in Fig. 10.

The projected characteristics passing the point P at the time $(p+1)\Delta t$ and the spatial location (l, m, n) then intersect the $p\Delta t$ axis at $Q_1, Q_2, \ldots, Q_7$. For $U_f > U_A > U_s > u > 0$, the projected characteristic PQ_1 can be identified with $dx/dt = u + U_f = \alpha^{(5)}$, so that PQ_2 with $dx/dt = u + U_A = \alpha^{(3)}$, PQ_3 with $dx/dt = u + U_s = \alpha^{(7)}$, PQ_4 with $dx/dt = u = \alpha^{(1)}$ and $\alpha^{(2)}$, PQ_5 with $dx/dt = u - U_s = \alpha^{(8)}$, PQ_6 with $dx/dt = u - U_A = \alpha^{(4)}$, and PQ_7 with $dx/dt = u - U_f = \alpha^{(6)}$.

Now let us consider the directional derivative of a physical variable w in the (x, t) plane along a line $s(x, t)$ characterized by

$$\frac{dx}{dt} = \alpha = -\frac{\partial s/\partial t}{\partial s/\partial x}$$

The differential derivative is

$$\frac{dw}{ds} = \frac{\partial w}{\partial t}\frac{\partial t}{\partial s} + \frac{\partial w}{\partial x}\frac{\partial x}{\partial s} = \mathbf{s} \cdot \nabla w \tag{A.2}$$

where s is the unit vector along $s(x, t)$, i.e.,

$$s = \left[\frac{\partial t/\partial s}{\sqrt{(\partial t/\partial s)^2 + (\partial x/\partial s)^2}}, \frac{\partial x/\partial s}{\sqrt{(\partial t/\partial s)^2 + (\partial x/\partial s)^2}}\right]$$
$$= \left[\frac{1}{\sqrt{1+\alpha^2}}, \frac{\alpha}{\sqrt{1+\alpha^2}}\right], \tag{A.3}$$

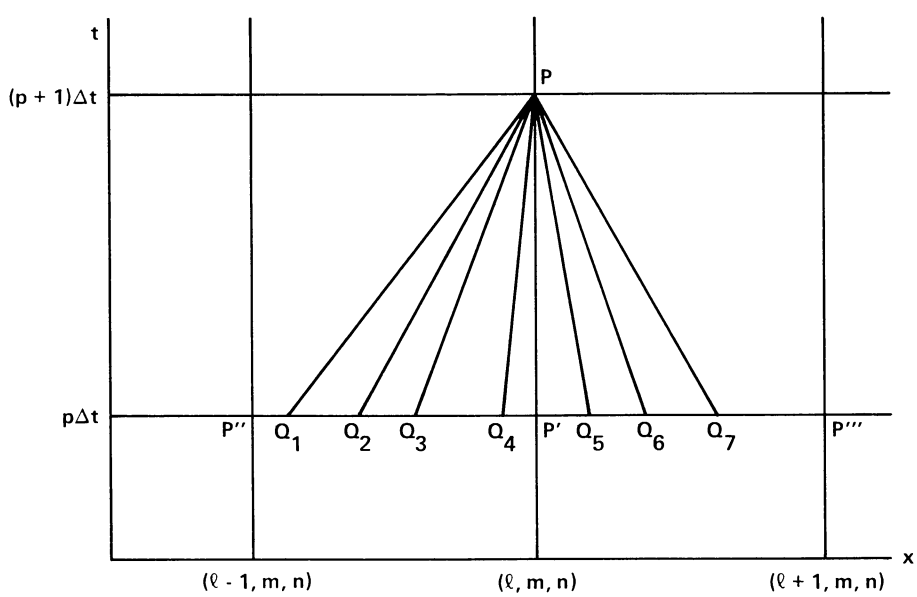

Fig. 10. The projected characteristics PQ_j $(j = 1, 2, \ldots, 7)$ in the (x, t)-plane, where the linearity is assumed for simplicity

and

$$\nabla w = \left[\frac{\partial w}{\partial t}, \frac{\partial w}{\partial x}\right], \tag{A.4}$$

Then from Fig. 10, the directional derivative dw/ds can be expressed, say for $\alpha = \alpha^{(5)}$,

$$\frac{dw}{ds} = \frac{w(p) - w(Q_1)}{PQ_1}$$

with

$$PQ_1 = [(PP')^2 + (Q_1P')^2]^{1/2} = \Delta t[1 + (\alpha^{(5)})^2]^{1/2}$$

and

$$w(Q_1) = w(P') - \frac{\partial w(P')}{\partial x} Q_1 P' + \dots$$

$$= w^p_{l,m,n} - \frac{(w^p_{l,m,n} - w^p_{l-1,m,n})}{\Delta x} \alpha^{(5)} \Delta t + \dots$$

Thus writing $w(p) = w^{p+1}_{l,m,n}$

$$\frac{dw}{ds} = \frac{1}{[1 + (\alpha^{(5)})^2]^{1/2}} \left[\frac{w^{p+1}_{l,m,n} - w^p_{l,m,n}}{\Delta t} + \alpha^{(5)} \frac{w^p_{l,m,n} - w^p_{l-1,m,n}}{\Delta x}\right]. \tag{A.5}$$

While the directional derivative defined by the last expression in Eq. (A.2) is

$$\frac{dw}{ds} = \boldsymbol{s} \cdot \nabla w = \frac{1}{[1 + (\alpha^{(5)})^2]^{1/2}} \left[\frac{\partial w}{\partial t} + \alpha^{(5)} \frac{\partial w}{\partial x}\right] \tag{A.6}$$

Comparing Eqs. (A.5) and (A.6), it is clear that along the characteristic $dx/dt = \alpha^{(j)}$, the directional derivative can be expressed in the following difference form at the time step $p\Delta t$ and grid point (l, m, n) for $\alpha^{(j)} > 0$,

$$\frac{\partial w}{\partial t} + \alpha^{(5)} \frac{\partial w}{\partial x} = \frac{w^{p+1}_{l,m,n} - w^p_{l,m,n}}{\Delta t} + \alpha^{(j)} \frac{w^p_{l,m,n} - w^p_{l-1,m,n}}{\Delta x}$$

and for $\alpha^{(j)} < 0$, the spatial derivative is replaced by

$$\alpha^{(j)} \frac{w^p_{l+1,m,n} - w^p_{l,m,n}}{\Delta x}$$

With this rule, the directional derivatives of $\partial \boldsymbol{W}/\partial x$ in the (x, t) plane can be expressed for $\alpha^{(j)} > 0$,

$$\frac{\partial \boldsymbol{W}}{\partial x} = \Delta^-_x \boldsymbol{W} = (\Delta_x \boldsymbol{W} - \delta_x \boldsymbol{W})$$

and for $\alpha^{(j)} < 0$,

$$\frac{\partial \boldsymbol{W}}{\partial x} = \Delta^+_x \boldsymbol{W} = (\Delta_x \boldsymbol{W} + \delta_x \boldsymbol{W})$$

where

$$\Delta^+_x \boldsymbol{W}_{l,m,n} = \frac{\boldsymbol{W}_{l+1,m,n} - \boldsymbol{W}_{l,m,n}}{\Delta x},$$

$$\Delta^-_x \boldsymbol{W}_{l,m,n} = \frac{\boldsymbol{W}_{l,m,n} - \boldsymbol{W}_{l-1,m,n}}{\Delta x}, \tag{A.7}$$

and

$$2\Delta_x \boldsymbol{W} = \Delta^+_x \boldsymbol{W} + \Delta^-_x \boldsymbol{W}, \qquad 2\,\delta \boldsymbol{W} = \Delta^+_x \boldsymbol{W} - \Delta^-_x \boldsymbol{W}. \tag{A.8}$$

The derivatives not contained in the (x, t) plane, i.e., $\partial \boldsymbol{W}/\partial y$ and $\partial \boldsymbol{W}/\partial z$, are then expressed in terms of the center differences as

$$\frac{\partial \boldsymbol{W}}{\partial y} = \Delta_y \boldsymbol{W}, \qquad \frac{\partial \boldsymbol{W}}{\partial z} = \Delta_z \boldsymbol{W}. \tag{A.9}$$

After rewriting the compatibility equations in such different forms, the term $\partial \boldsymbol{W}/\partial t$ in the (x, t) plane is determined by solving the eight compatibility equations as a system of simultaneous algebraic equations for the eight components of $\boldsymbol{W}$. Then assembling the terms of spatial differences as defined in Eq. (A.8), we find the term of the type $\boldsymbol{D}\delta_x \boldsymbol{W}$ results. Repeating exactly the similar procedures in the (y, t) and (z, t) planes, the final form of equation becomes the form of Eq. (32). The factor $\frac{1}{3}$ in the matrices, therefore, simply signifies the averaging of the three directions.

It should be noted that in Eq. (32) the time derivative is represented by

$$\frac{\partial \boldsymbol{W}}{\partial t} = \frac{\boldsymbol{W}^{p+1}_{l,m,n} - \boldsymbol{W}^{*p}_{l,m,n}}{\Delta t}$$

This replacement of $W^p_{l,m,n}$ by $W^{*p}_{l,m,n}$ is done in consideration of the numerical stability.

Appendix B

The general rule of expressing the partial differentials in terms of finite differences remains similar to that given in the Appendix A. However, on the boundary surfaces of the domain of computation some modifications become necessary and those modifications are summarized below. At the time step $p\Delta t$ and spatial position (l, m) the temporal variation is expressed by

$$\Delta_t \boldsymbol{W}^p_{l,m} = \frac{\boldsymbol{W}^{p+1}_{l,m} - \boldsymbol{W}^{*p}_{l,m}}{\Delta t} \tag{B1}$$

where, on the boundary surface $x = L$,

$$\boldsymbol{W}^{*p}_{L,m} = \frac{\boldsymbol{W}^p_{L,m+1} + \boldsymbol{W}^p_{L,m-1}}{2},$$

on the boundary surface $z = M$,

$$\boldsymbol{W}^{*p}_{l,M} = \frac{\boldsymbol{W}^p_{l+1,M} + \boldsymbol{W}^p_{l-1,M}}{2},$$

and at the intersections of boundary surfaces, $x = L$ and $z = M$,

$$\boldsymbol{W}^{*p}_{L,M} = \boldsymbol{W}^p_{L,M}. \tag{B2}$$

Similar changes become necessary for the spatial derivatives. On the boundary surface $x = L$ the derivative not contained in the (x, t) plane is represented as follows (suppressing the time step index and asterisk),

$$\frac{\partial \boldsymbol{W}}{\partial z_{L,m}} = \Delta_z \boldsymbol{W}_{L,m} = \frac{\boldsymbol{W}_{L,m+1} - \boldsymbol{W}_{L,m-1}}{2\Delta z} = \frac{\Delta^+_z \boldsymbol{W}_{L,m} + \Delta^-_z \boldsymbol{W}_{L,m}}{2}. \tag{B3a}$$

Then for the derivatives contained in the (x, t)-plane, with the grid point $(L + 1, m)$ located inside of the domain of analysis,

$$\frac{\partial \boldsymbol{W}}{\partial x_{L,m}} = \Delta^+_x \boldsymbol{W}_{L,m} = \frac{\boldsymbol{W}_{L+1,m} - \boldsymbol{W}_{L,m}}{\Delta x}, \tag{B3b}$$

and with the point $(L-1, m)$ located in the domain of analysis,

$$\frac{\partial W}{\partial x_{L,m}} = \Delta_x^- W_{L,m} = \frac{W_{L,m} - W_{L-1,m}}{\Delta x} \tag{B3c}$$

In the similar manner, on the boundary surface $z = M$, the x-derivative is given by

$$\frac{\partial W}{\partial x_{l,M}} = \Delta_x W_{l,M} = \frac{\Delta_x^+ W_{l,M} + \Delta_x^- W_{l,M}}{2} \tag{B4a}$$

For the point $(l, M+1)$ located in the domain of analysis, the z-derivative becomes

$$\frac{\partial W}{\partial z_{l,M}} = \Delta_z^+ W_{l,M} = \frac{W_{l,M+1} - W_{l,M}}{\Delta z}, \tag{B4b}$$

and for the point $(l, M-1)$ located in the domain of analysis,

$$\frac{\partial W}{\partial z_{l,M}} = \Delta_z^- W_{l,M} = \frac{W_{l,M} - W_{l,M-1}}{\Delta z}. \tag{B4c}$$

It follows from these definitions of the spatial derivatives that on the boundary surfaces, the quantity $\delta_x W = (\Delta_x^+ W - \Delta_x^- W)/2$ can result only on the boundary surface $x = L$, and similarly, $\delta_z W = (\Delta_z^+ W - \Delta_z^- W)/2$ on the boundary surface $z = M$. Therefore, it is evident that in the final boundary equations, the term $\delta_x W$ appears with $\Delta_x W$, and either $\Delta_z^+ W$ or $\Delta_z^- W$ on the boundary surface $x = L$. Then the term $\delta_z W$ appears with $\Delta_z W$, and either $\Delta_z^+ W$ or $\Delta_x^- W$ on the boundary surface $z = M$. Further, it should be noted that at the point of intersections of boundary surfaces, the spatial derivatives in the boundary equation are confined only to the one-sided differences, such as, $\Delta_x^+ W$, $\Delta_x^- W$, $\Delta_z^+ W$, and $\Delta_z^- W$.

References

Akhiezer, A.I., Akhiezer, I.A., Polovin, R.V., Sitenko, A.G., Stepanov, K.N.: 1975, *Plasma Electrodynamics*. 1. Pergamon Press. Chap. 3

Han, S.M., Wu, S.T., Nakagawa, Y.: 1982, Computers & Fluids, **10**, 159

Hu, Y.Q., Wu, S.T.: 1984, *J. Comp. Phys.* **55**, 33

Jeffrey, A., Taniuti, T., 1964, *Non-Linear Wave Propagation*, Academic Press, Chaps. 1 and 3

Kneer, R., Nakagawa, Y.: 1976, *Astron. Astrophys.* **47**, 65

Low, B.C.: 1977, *Astrophys. J.* **212**, 234

Nakagawa, Y.: 1980, *Astrophys. J.* **240**, 275

Nakagawa, Y.: 1981a, *Astrophys. J.* **247**, 707

Nakagawa, Y.: 1981b, *Astrophys. J.* **247**, 719

Richtmyer, R.D., Moreton, K.W.: 1976, *Difference Method for Initial Value Problems*, Interscience, New York, Chap. 12

Sauerwein, H.: 1966, *J. Fluid Mech.* **25**, 17

Shin, Y.W., Kot, C.H.: 1978, *J. Comp. Phys.* **28**, 211

Wu, S.T., Hu, Y.Q., Nakagawa, Y., Tandberg-Hanssen, E.: 1983, *Astrophys. J.* **266**, 866

Wu, S.T., Hu, Y.Q., Krall, K.R., Hagyard, M.J., Smith, Jr., J.B.: 1984, *Solar Physics* **90**, 117–131

Wu, S.T., Hu, Y.Q., Nakagawa, Y., Tandberg-Hanssen, E.: 1986, *Astrophys. J.* **306**, 751